GENE TRANSFER FOR THE TREATMENT OF NEOVASCULAR OCULAR DISEASE (AN AMERICAN OPHTHALMOLOGICAL SOCIETY THESIS)

BY John Timothy Stout MD PhD MBA

ABSTRACT

Purpose: As vasoproliferative diseases account for a substantial fraction of worldwide blindness and share the activation of the angiogenic pathway as a common etiology, the expression of antiangiogenic proteins offers a promising means of treatment. This study was designed to develop viral vectors, harboring angiostatic genes, for the study and treatment of experimental proliferative ocular disease. A variety of methods (in vitro, ex vivo tissue, and in vivo) were employed to model the process of proliferation and test the effectiveness of these reagents.

Methods: Antiangiogenic genes included single genes as well as hybrid genes that fused the active elements of different genes. Genes studied included the soluble vascular endothelial growth factor receptor (*sKDR*), soluble neuropilin (*sNRP-1*), tissue inhibitor of metalloproteinase-1 (*TIMP-1*), plasminogen gene fragments (Kringle 1-3, 1-4, and 1-5), and soluble receptors for advanced glycosylation end products (*sRAGE*) genes, as well as the *Endo:Ang*, *MIG:IP10*, and Endo:Kringle5 fusion genes. All genes were cloned into a lentiviral vector system and were used to produce replication deficient lentiviral particles. These viral particles were used to transduce a variety of ocular cells and tissues to test viral transfer efficiency and transgene expression. In vivo systems were employed to explore the potential of these genes as antiangiogenic agents in models of corneal and retinal neovascular disease.

Results: Recombinant lentiviral particles, capable of transducing cell lines germane to eye disease (ocular endothelial, epithelial, and fibroblast cells), were successfully produced. These vectors were demonstrated to be effective in long-term transformation of cells and tissues. In vivo experiments confirmed that at least three different potentially angiostatic genes were successful in aborting the angiogenic process in the ocular models tested.

Conclusions: Lentiviral vectors are a viable means to deliver angiostatic genes to tissues of the eye. Some angiostatic genes appear to have a stronger and longer-lasting effect than others in modulating the angiogenic pathway.

Trans Am Ophthalmol Soc 2006;104:530-560

INTRODUCTION

Much of blindness in the developed world is associated with a limited number of ocular diseases. Whereas aging, inflammation, metabolic imbalance, infection, and trauma contribute to these pathologies, the proliferative neovascular response often represents a common pathologic feature. Angiogenesis, the process of development and differentiation of new blood vessels, is a normal, regulated process perhaps most recognized for its role in development and a wide variety of "wound healing" responses. Processes such as menstruation and tissue remodeling are dependent on a balance between proangiogenic and antiangiogenic factors. Imbalance between these factors leads to disease: a significant decrease in angiogenic factors is associated with disease processes like stroke, infertility, and heart disease, whereas overstimulation of the angiogenic process is associated with diverse diseases such as arthritis, cancer, and neovascular ocular disease.

Neovascular diseases of the eye affect a number of distinct tissue types, including the retina and the cornea. Retinopathy of prematurity (ROP), age-related macular degeneration (AMD), proliferative diabetic retinopathy (PDR), and retinal vaso-occlusive (RVO) disorders disorders are disparate disease processes that share a common risk of robust, pathological neovascularization.

ROP is a two-stage disease; the first stage is initiated by standard post birth oxygen therapy, which results in cessation of normal vasculogenesis, thus rendering a portion of the retina avascular. The second stage of disease is caused by the return to a normoxic environment which stimulates an ischemic response. Retinal ischemia reinitiates the expression of factors such as vascular endothelial growth factor (VEGF) resulting in aberrant blood vessel formation and subsequent retinal detachment.

The exudative form of AMD is a multifactorial disease with both environmental and genetic associations. Although the etiologies are unknown, central vision loss with subretinal neovascularization is a final common pathway in patients over the age of 60 years. Potential relationships between inflammation, infectious disease, ischemia, and changes within extracellular matrices and subretinal neovascularization are under intensive study.

Similar to patients with ROP, a significant ocular complication in patients with diabetes mellitus is the neovascular response to retinal ischemia. This disease is pathologically associated with the breakdown of the blood-retinal barrier, vascular permeability, and neovascularization. An additional group of diseases that are pathologically related to retinal ischemia are the vaso-occlusive processes that can involve either retinal arteries or veins. Occlusions may occur in the central retinal artery (CRAO), central retinal vein (CRVO), or the branch segments of the vascular bed (BRAO or BRVO). The lack of blood flow initiates the process of ischemia and results in an increased risk of neovascular disease.

Corneal neovascular disease is usually associated with local inflammation (traumatic or infectious) and remains the most common

reason for graft rejection following penetrating keratoplasty (PKP), the most common transplant surgeries performed in the United States.[1] Whether there are common and/or different inciting factors in corneal neovascularization compared with retinal neovascularization is under study.

Current interventions for proliferative ocular disease are based largely on techniques such as laser or cyro ablation of tissue, photodynamic therapy, or surgical techniques that mechanically address the tractional forces associated with neovascular disease. Although these treatments are often successful in halting disease progression, they are destructive and are usually not restorative. As our understanding of the proteins and small molecules that influence angiogenesis increases, so do our options for treatment. This complex pathway is not entirely understood, but recent advances in genomics and proteomics have identified many of the key initiators of angiogenesis. Modulating the cascade of molecular events within the angiogenic pathway may offer a means to this therapeutic end.

ANGIOSTATIC GENES

Control of genes able to inhibit or down-regulate angiogenesis has great therapeutic potential. There are several classes of antiangiogenic genes; these are generally categorized by their mode of action. Inhibitors of matrix metalloproteinases, a large class of endopeptidases, and specifically tissue inhibitors of metalloproteinases (*TIMPs*) have been shown to degrade extracellular matrix components, which inhibits cellular morphogenesis.[2,3] This is of interest because endothelial cell migration and formation of the tube structures, which comprise blood vessels, are dependent upon cellular scaffolding for structural stability. *TIMP-1* has been demonstrated to inhibit the process of vascular remodeling in vitro, and overexpression of this gene shows potential for destabilizing vessel differentiation.[4] In an experimental transgenic mouse model of hepatocellular carcinoma, *TIMP-1* overexpression was shown to block formation of carcinomas by inhibiting cellular growth and angiogenesis.[5]

Receptors that bind molecules known to stimulate angiogenic cascades offer a second therapeutic strategy. Soluble isoforms of these receptors can bind and deactivate extracellular stimuli before they can bind to the active cellular membrane-bound complement receptors to invoke a cellular response. VEGF receptors such as kinase domain receptor (KDR) and the coreceptor neuropilin-1 (Nrp-1) bind VEGF at two separate sites on the molecule.[6] When these receptors are coexpressed on the same cell or expressed singly on adjacent cells, VEGF-induced angiogenesis is up-regulated up to sevenfold.[6] Evidence suggests that overexpression of these receptor molecules in the soluble form inhibits VEGF from reaching its membrane-bound constituent, thus shielding the cells from VEGF stimulation. The receptor known to bind advanced glycosylation end products (AGE), formed when blood sugar is abnormally elevated in cases of unmanaged diabetes, has been shown to initiate apoptosis in pericytes and enhance VEGF production in endothelial cells.[7,8] Pericytes are cells that sheath blood vessels, providing vascular tube stability. When the integrity of these cells is undermined, they perish and the associated vasculature becomes leaky. Often with concomitant endothelial cell stimulation by VEGF, neovascularization ensues. The potential to block membrane-bound receptors from interacting with extracellular AGE by-products using soluble docking systems may prove effective at reducing the sequelae associated with PDR.

Other proteins are able to specifically inhibit endothelial cell differentiation and VEGF stimulation. These proteins can prevent endothelial cells from migrating and forming the secondary structures required for proliferation and vessel formation. Endostatin and plasminogen (specifically the cleaved angiostatin and the kringle domain products) have both been demonstrated to possess these properties. Endostatin, the carboxy-terminal end of the collagen XVIII protein, is a potent inhibitor of endothelial cell proliferation and migration.[9,10] Endostatin can specifically down-regulate genes such as *c-fos*, *c-myc*, *MAPK-1*, *MAPK-2*, *bcl-XL*, *bcl-2*; integrins, and cadherin-5, all of which are involved in cell growth and antiapoptotic and angiogenic processes.[11-13] Endostatin has also been reported to inhibit cell matrix adhesion in endothelial cell as well as promote G_1 arrest through the inhibition of cyclin D1.[14] Angiostatin and the kringle domains 1-5 are known to inhibit tumor growth by specifically inhibiting endothelial cell migration and vascular tube formation mediated by binding to angiomotin, a protein that is found localized to the leading edge of lamellipodia of migrating cells. In vitro experiments show that angiostatin is bound and internalized by angiomotin and, subsequently, both proteins are found localized within vesicles.[15] The kringle domains; K1-3, K1-4, and K1-5 are known to induce apoptosis in bovine adrenal cortex derived capillary endothelial and bovine aortic endothelial cells.[16] Although the exact mechanism of the antiangiogenic action is not known, studies suggest that angiostatin and the cleaved kringle domains may prevent new blood vessels from forming by inducing endothelial cell specific apoptosis and inhibiting endothelial cell migration.

Inhibition of the chemotactic signals, which stimulate cells to migrate and induce production of proinflammatory and proangiogenic products, is valuable in down-regulating early events within the angiogenic cascade. The chemokines interferon-alpha inducible protein 10 (IP10) and monokine-induced by interferon-gamma (MIG) are small, secreted proteins that contribute to chemotaxis and regulate cell growth, are related in structure, and share the same CXC receptor for cellular activation.[17] Both MIG and IP-10 are characterized as having the following properties: inhibition of cellular colonization, T-cell activation and cytolysis, and antiangiogenic effects by tube formation disruption.[18,19]

Given that many of the aforementioned genes are either derived from the same progenitor protein (angiostatin and the kringle domains) or act synergistically and/or via similar pathways (MIG and IP-10), it may be useful to consider using two genes to act on independent pathways simultaneously to form bifunctional fusion proteins. Fusion genes can be engineered to contain the active protein motifs of two genes, which are linked by neutrally charged amino acids (ie, the elastin motif) that will not contribute to the overall secondary structure of the recombinant protein nor disrupt the function of either protein moiety.[20] The use of fusion genes is a promising strategy that could potentially be a more powerful alternative than individual genes used alone.

GENE DELIVERY

Selection of candidate genes that modulate the process of angiogenesis is one step in the development of a therapeutic approach. Another factor requiring careful consideration is how to direct efficient delivery of these genes into specific cells or tissues. There are several means by which genes can be delivered to cells, including physical, chemical, and virus-mediated techniques. Each option offers it own intrinsic limitations, benefits, and concerns.

Physical delivery of genes is accomplished by a number of techniques ranging from direct injection of plasmid DNA to the use of pneumo-ballistic guns, which "shoot" DNA deep into tissues. One common chemical-mediated delivery system employs cationic lipids or polymers that envelope the DNA during delivery. Physical and chemical delivery systems have disadvantages: tissue specificity is poor, and transgene expression is often nominal and transient. These problems may be due to the rapid degradation of the introduced DNA (seen less with chemical methods) and damage to target cellular membranes.[21,22]

Viral-mediated gene delivery has traditionally been felt to be a reliable means of transgene introduction as viruses have evolved over many years to accomplish efficient transgene insertion and expression. The three classes of viruses most widely used for gene therapy include the adenoviridae (Ad), the adeno-associated viruses (AAV), and retroviruses (mainly oncoretroviruses and lentiviruses).

Adenoviruses are nonenveloped iscosahedral particles with large double stranded DNA genomes approximately 36 kb in size.[23] They have the capability of infecting cells both in G0 and in S phase and offer strong, short-term transgene expression.[24] A drawback to these vectors is that they are incapable of genomic integration, resulting in transient transgene expression, and may require multiple vector administrations to achieve therapeutic benefit in chronic disease states. In addition, these vectors have been associated with strong humoral immune effects, complicating their safety profile.[25]

Adeno-associated viruses are small single-stranded DNA-containing particles. They offer the capability of genomic integration, thus long-term transgene expression, and can infect both dividing and stationary cells.[26] A limitation of AAV vectors is that their genome size is quite small, less than 5 kb.[27] The small carrying capacity of this vector makes gene selection difficult, particularly for the study of therapies that employ large receptor-encoding genes.

Retroviral-mediated transduction has a long history of intensive study. Oncoretroviruses, while enjoying a relatively large carrying capacity, suffer from an inability to infect the nondividing cells that comprise most of the human eye.[28] Lentiviral vectors can transduce both dividing and nondividing cells and, as integrating vectors, support long-term transgene expression.

LENTIVIRAL PROPERTIES AND RATIONALE FOR USE

Lentiviral vectors are derived from the human immunodeficiency virus (HIV-1) and have been extensively studied for the use as a vehicle for gene transfer. These vectors are capable of transducing quiescent cells (a likely requirement for ocular gene therapy), they offer integrative capabilities resulting in long-term stable transgene expression, and they have not been associated with a robust immune response.

Lentiviruses are enveloped viral particles composed of matrix proteins (including Gag), fragments of the host's cell membrane (obtained through the budding process), and glycoprotein knobs (ENV) (used for attachment and entry into target cells). The lentiviral core consists of a diploid single-stranded RNA genome and the enzyme reverse transcriptase (Pol), which allows the lentiviral genetic material to be made into double-stranded DNA, providing the ability for chromosomal insertion via long terminal repeat (LTR)-mediated integrative events.[29] Unlike retroviruses, lentiviruses possess many accessory genes, such as *Tat, Rev, VPU, VIF, VPR* and *NEF*, which increase cell cycle tropism, replication, and release. These accessory genes increase virulence and are required for efficient wild-type propagation. Tat is responsible for viral promoter activation in the LTR, leading to efficient gene transcription. The rev protein, by interaction with the rev responsive element (RRE), facilitates transport of viral transcripts from the nucleus to the cytoplasm. Viral protein undefined (VPU) is responsible for facilitating ENV maturation and viral release. Viral infectivity factor (VIF) interferes with the cells' antiviral defense and is necessary for proper viral assembly. Viral protein R (VPR) arrests the cell cycle and promotes nuclear localization. Negative factor (NEF) prevents a cell from inducing the apoptotic pathway and increases viral reverse transcription.[30]

Identification of the above accessory genes has led to development of a delivery vehicle that is far safer than the wild-type virus. By removing *VIF*, *VPR*, *VPU*, and *NEF*, lentiviral vectors are capable of infecting cells but do not elicit the cellular effects associated with these proteins. Another modification to lentiviruses was to switch the wild-type glycoprotein (ENV) with that of the vesicular stomatitis virus (VSV) glycoprotein. This accomplishes two things: it widens the cellular tropism of the virus to infect more cell types, and it makes the virus heavier, aiding in recombinant viral isolation procedures.[31] Another modification to the virus separates the required genes into three different plasmids and produces recombinant particles by transient transfection methods in virus assembly cells in vitro. This permits the manufacture of recombinant viral particles that are replication-deficient, thus increasing the safety of the vector. Finally, modifications (self-inactivating [SIN] modifications) that delete the enhancer region of the 3′ U3 of the long terminal repeat (LTR) result in a transcriptionally inactive vector that cannot be converted into a full-length RNA, thus reducing the likelihood of replication competency and hampering the mobilization of wild-type HIV in HIV-infected recipients (Figure 1).

Despite the fact that these modifications have produced lentiviral vectors with few adverse target cell effects, key safety concerns persist. The integrative nature that makes these vectors attractive for long-term transgene expression also makes them potentially harmful. Integration into areas of the genome, perhaps into areas that would up-regulate proximal oncogene expression or integration into the middle of tumor suppressor genes, could give rare target cells unwanted growth and survival characteristics.[32] The treatment of children with severe combined immunodeficiency (SCID) with non-SIN retroviral vectors led to insertional mutagenic changes that

caused hematopoietic neoclassic and has suggested that the insertion of retroviral sequences into the genome carries significant risk.[33] Concern about the possibility of *cis*-activation of genes near the site of integration has thus been addressed by the design of SIN vectors. Continued manipulation of this vector to improve the safety for human use is ongoing. The use of lentiviral vectors for gene therapy offers an elegant means for transgene delivery, especially to the relatively compartmentalized eye.
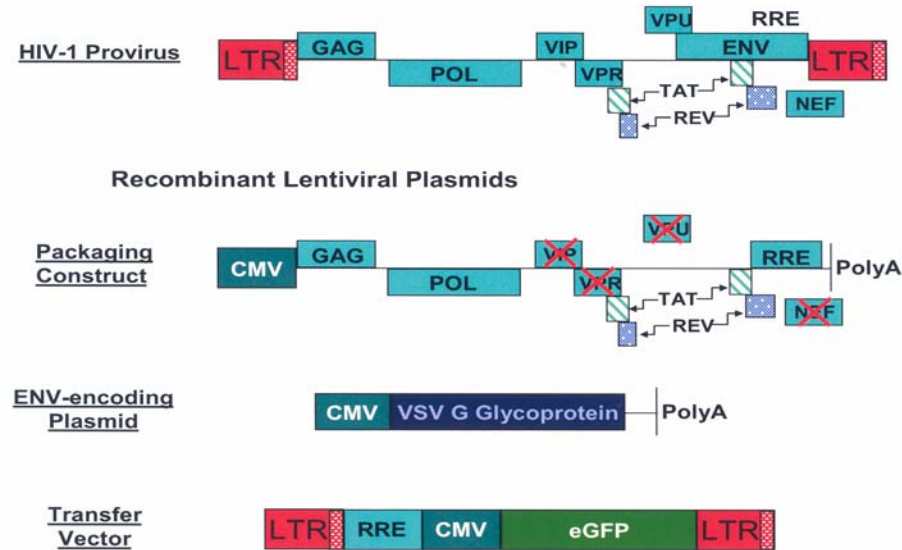

FIGURE 1

Lentiviral constructs. Schematic illustrating the genes of wild-type HIV-1 and recombinant lentiviral vector constructs used for viral production.

PRESENT STUDY

Hypothesis

Angiostatic genes delivered to retinal and corneal tissues via lentiviral vectors inhibit neovascularization both in vitro and in animal models of proliferative ocular disease.

Aim

A lentiviral vector harboring the marker gene green fluorescent protein was used to assess the long-term transgene expression in several ocular cell lines. The angiostatic genes—*endostatin-angiostatin* fusion gene, *MIG-IP10* fusion gene, *sKDR*, *TIMP-1*, *sNRP-1*, *kringle 1-5* of *plasminogen*, *endostatin-kringle 5* fusion, *sRAGE*—were cloned into a lentiviral vector and evaluated for antiangiogenic affects in several cellular assays as well as in vivo experiments using rabbit and nonhuman primate systems. Corneal angiogenesis and subretinal neovascularization models was examined.

METHODS

All experimentation was conducted under approved institutional review board, biosafety, and animal care (IACUC) protocols. These protocols conformed in entirety with guidelines approved by the Association for Research in Vision and Ophthalmology.

PLASMID PREPARATION

eGFP

The plasmid pHR-CMV-ires-eGFP was a kind gift from the laboratory of Didier Trono and is the vector into which all angiostatic genes included in this study were cloned (Figure 2). Primers used for cloning and corresponding restriction enzymes are given in Table 1. This lentiviral vector may be acquired via application through http://tronolab.com/.

Endo-Ang

The fusion gene encoding 20 amino acids of the human interleukin-2 secretion signal, 184 amino acids of human endostatin XVIII, an elastin peptide linker, and 365 amino acids of angiostatin (corresponding to kringle domains 1-4) was polymerase chain reaction (PCR) amplified from the pBlast-Endo: Kringle5 vector (Invivogen Inc, San Diego, California).

MIG-IP10

The fusion gene encoding the first 127 amino acids of the monokine-induced by interferon-gamma (Mig) protein and the 79 amino acids of the interferon alpha-inducible protein 10 protein, linked by the elastin motif, was PCR amplified from the pBlast-MIG:IP10 vector (Invivogen Inc).
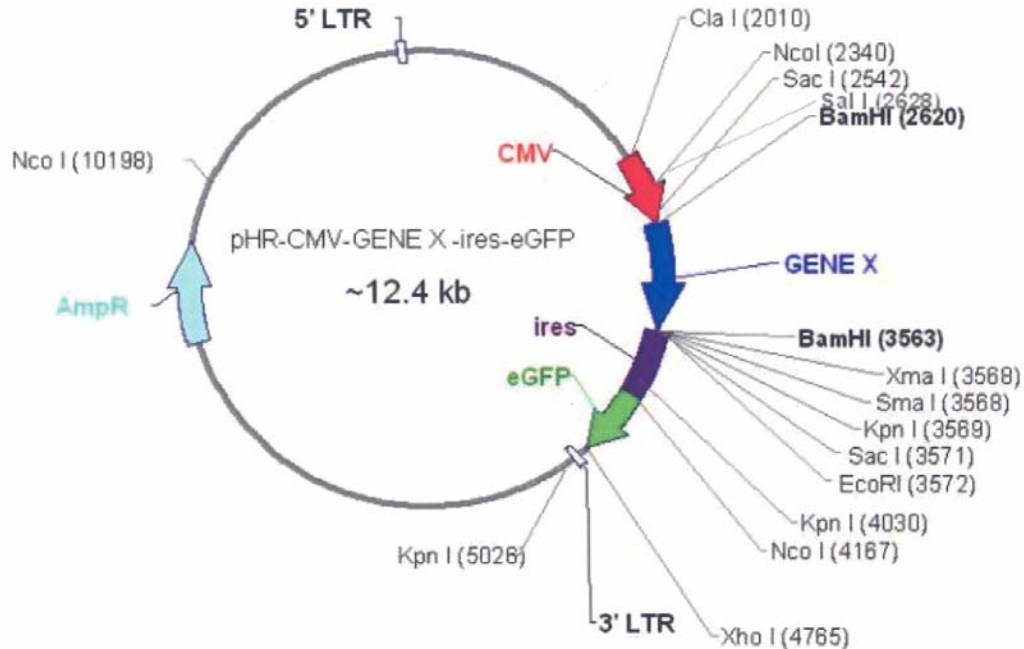
FIGURE 2

Cloning vector. Plasmid map of lentiviral vector containing the cytomegalovirus (CMV) promoter, Transgene (GENE X), internal ribosomal entry site (ires), and the enhanced green fluorescent protein (eGFP) cDNA. Map was created with Redasoft Visual Cloning 2000.

sKDR

The cDNA encoding the soluble VEGF receptor 2, also termed kinase domain receptor (sKDR), was PCR amplified from the pBlast-sKDR vector (Invivogen Inc).

Timp-1

The cDNA encoding the first 207 amino acids of the tissue inhibitor of metalloprotease (Timp1) was PCR amplified from the pBlast-Timp-1 vector (Invivogen Inc).

K1-5

The cDNA coding for the 452 amino acids of K1-5 was PCR amplified from the pBlast-K1-5 vector (Invivogen Inc).

EK5

The cDNA coding for the 183 amino acids of endostatin and 100 amino acids of the kringle 5 domain of angiostatin was PCR amplified from the pBlast-EK5 vector (Invivogen Inc).

sNRP-1

DNA sequence corresponding to the 645 amino acid, soluble form of Nrp-1 was PCR amplified from the pOTB7-sNRP-1 vector (ResGen Inc).

sRAGE

The full-length cDNA of RAGE (ResGen) was modified by PCR to the 351 amino acid soluble form by using a reverse primer that contained the 3′ sequence of soluble RAGE.

PCR products and pHR plasmids were digested with the appropriate restriction enzymes, separated by electrophoresis on a 0.8% agarose gel, column purified (Zymogen Inc), and ligated together by incubation in 1X ligation buffer containing T4 DNA ligase (Fermentas Inc) at room temperature for 30 min. 3 μL of the ligation mix was used to transform DH5α competent *Escherichia coli* cells (Invitrogen Inc). The *E coli* preparations were grown in a 37°C orbital shaker incubator with 900 μlL of SOC media for 1 hour. 200 μL of the *E coli* was spread onto LB-ampicillin agar plates and incubated overnight at 37°C. Individual colonies were harvested and mini-prep plasmid isolation was performed (Promega Inc). Ligation was verified by digestion of the purified plasmid DNA with the same enzymes used for cloning and was separated by standard gel electrophoresis for visualization and confirmation.

SEQUENCING

Sequencing was performed to verify that plasmid constructs were correctly prepared. This was performed using the ABI 310 genetic analyzer following manufacturer's recommendations. Briefly, PCR reactions were set up to contain the following: 1 μg of the above angiostatic pHR vectors, 4 μL of BigDye version 3.1 (ABI Inc), 4 μL of sequencing primer (0.8 pmol) and water to a final volume of 20 μL. Amplification consisted of 35 cycles of 96°C for 10 seconds, 52°C for 10 seconds, and 65°C for 2 minutes. DNA was precipitated with 50 μL of 95% EtOH and 2 μL of 3M NaAc, which was incubated on ice for 20 minutes followed by 30-minute centrifugation at 15,000 rpm. The DNA pellet was washed twice in 70% EtOH and air-dried at room temperature. The dried pellet was suspended in 12 μL of Template suspension reagent (TSR, ABI Inc) and loaded onto the sequencing apparatus. Sequences were analyzed using Chromas software (Technelysium Pty Ltd). All sequencing primers were designed to amplify both strands and were separated by 300 bp (sequences available upon request).

VIRUS PRODUCTION

Recombinant lentiviral vectors were produced by transient cotransfection in 293T cells (ATCC). 15 μg of pHR plasmid containing an angiostatic gene was mixed with 15 μg of delta R8.91 plasmid and 3.5 μg of VSV-G plasmid. Hepes buffered saline (HBS - 137mM NaCl, 5mM KCl, 0.7mM Na2HPO4, 6mM dextrose, 21mM HEPES pH 7.4) was added to a final volume of 500 μL. 32 μL of 2M CaCl$_2$ was added dropwise, and the contents were mixed by gentle vortexing. The mixture was incubated at room temperature for 45 minutes. The plasmid mixture was then added to 80% confluent 293T cells plated in 75 cm2 tissue culture flasks, incubated for 10 minutes at room temperature, gently rocked and incubated for an additional 10 minutes. Ten mL of DMEM 10% FBS was added to the plates and incubated in a tissue culture incubator overnight at 37°C 5% CO2. The following day, media was replaced with fresh DMEM 10% FBS containing 10mM NaButyrate and 20mM HEPES and placed back into the incubator for 24 hours. The media was replaced with fresh DMEM 10% FBS 20mM HEPES and incubated as before for 24 hours. This media was collected and replaced with fresh DMEM 10% FBS 20mM HEPES and again returned to the incubator for 24 hours; this was repeated for 2 to 3 days. The collected media was pooled, filtered through a 0.8-micron filter, and viral particles were concentrated by ultracentrifugation at 14,000 rpm at 4°C for 3.5 hours. The media was carefully removed and the viral pellet was resuspended in 200 μL of phosphate-buffered saline (PBS) by gentle rocking overnight at 4°C.

ANALYSIS OF VIRAL VECTOR

ELISA

Sandwich ELISA for P24 GAG of HIV-1 (Zeptometrix Inc) was performed to quantify recombinant viral particle concentration. 1 μL of the viral preparation was mixed with 449 μL of PBS, to which 50 μL of lysing reagent was added. 200 μL of the mixture along with the provided P24 standard (ranging from 1 to 50 pg) was added to a 96-well P24 ELISA plate and incubated for 1 hour at 37°C; all samples were tested in duplicate. The wells were washed four times with 1× wash buffer and patted dry onto paper towels. The 100 μL of the substrate conjugated P24 antibody was added to the plate and incubated for 1 hour at 37°C. The plate was washed again as before. 100 μL of substrate was added to the plate and allowed to develop for 5 minutes. The plate was analyzed using a colorimetric plate reader using a 450-nm filter. A standard curve was generated and the viral concentration was estimated using the ratio: 200 pg P24 equaled 1×10^8 viral particles (information supplied by Zeptometrix); data was then adjusted for the dilution factor.

Transduction and RNA Isolation

Viral particles were assessed for infectivity and transgene expression by microvascular endothelial cell (MVEC) transduction assay. 1×10^4 MVECs (Cascade Biologicals Inc) were seeded into 6-well plates supplied with Media 131 containing growth supplement (Cascade Biologicals Inc) and allowed to establish for 24 hours at 37°C 5% CO2. 1×10^8 particle units (pu) of virus was added to the wells and incubated for 3 days to ensure efficient transgene expression. Cells were viewed by fluorescent microscopy to verify green fluorescent protein expression. Media was removed and the cells were washed twice with PBS. 50 μL of lysis buffer was added to the cells and RNA was isolated using column purification methods (Ambion Inc). RNA was quantified using standard OD 260 spectrophotometric analysis.

RT-PCR

Reverse transcriptase PCR was performed to verify the presence of viral mediated mRNA transcripts. Reverse transcription was facilitated by adding 50 μg of RNA to 4 μL of 5X RT buffer, 1 μLof reverse transcriptase (Bio-Rad Inc), and water to a final volume of 20 μL. RT parameters were 25°C for 10 minutes, 45°C for 30 minutes, and 85°C for 15 minutes. PCR reactions contained 10% of the RT mix, 2.5 μL PCR buffer containing 15mM MgCl$_2$ (Sigma Inc), 0.5 μL 10mM dNTPs, 1 μL RedTaq polymerase (Sigma Inc), 1 μL of forward primer (20 pmol), 1 μL of reverse primer (20 pmol) and water to a final volume of 25 μL. The PCR conditions were as follows: 25 cycles of 95°C for 30 seconds, 50°C for 30 seconds, and 72°C for 30 seconds. PCR reactions were performed for the angiostatic gene of interest as well as for β-actin, to confirm the presence of in tact RNA (primer sequences provided upon request). PCR reactions were separated on a 1% agarose gel by electrophoresis and visualized by ethidium bromide staining.

IN VITRO EXPERIMENTATION

Iris Pigment Epithelial (IPE) Isolation

Primary culture of IPE cells was established from human donor eyes (Lions Eye Bank, Portland, Oregon) and from Norwegian Brown rat eyes. Iris tissue was dissected from the limbus and placed in a Petri dish with the anterior surface down. The tissue was washed twice with Hanks Balanced Salt Solution (HBSS). IPE cells were harvested with the use of fine forceps under a dissecting microscope after a 30-minute incubation in 0.25% Trypsin at 37°C. The isolated IPE cells were seeded into 6-well plates containing F-12 media (Gibco Inc) supplemented with 20% FBS.

Retinal Pigment Epithelial (RPE) Isolation

Human eyes were obtained from the Anatomic Gift Foundation. RPE cells were isolated by dissecting the eye 2 to 3 mm away from the sclerocorneal edge. Vitreous was removed and the retina was peeled away from the eyecup. The eyecup was placed in PBS containing 2% dispase (Gibco Inc) for 50 minutes at 37°C. After incubation, Bruch's membrane with attached RPE cells was scraped off using an inoculation loop, cut into small pieces, collected by centrifugation, and plated into laminin-coated 6-well plates. The RPE cells were cultured in high glucose DMEM supplemented with 10% FBS.

Choroidal Fibroblasts (CF) Isolation

CF cells were collected from the same eyecup as the RPE cells by direct dissection. The tissue was cut into small pieces and seeded into a 6-well plate and cultured in DMEM-high glucose supplemented with 10% FBS.

Corneal Cell Isolation

Corneal tissue was obtained either through the Anatomic Gift Foundation or the Los Angeles or Portland Lions Eye Banks. Surrounding tissues were removed; the eye was bisected 2 to 3 mm away from the sclerocorneal edge. The sclerocorneal section was washed by HBSS and the sclera was excised under a stereomicroscope, and the endothelium, together with Descemet's membrane, was peeled off with jeweler's forceps. The epithelial and stromal layers were incubated in HBSS containing 2% dispase (Gibco) at 37°C for 50 minutes, and the corneal epithelium was scraped off by an inoculating loop. The stromal layer was cut into small pieces and cultivated in a flask with DMEM, containing 20% FBS. When the corneal keratocytes and epithelial cells proliferated to confluency, cells were passed and cultured in 10% FBS DMEM. In vitro transduction experimentation of corneal endothelial cells was conducted with cells attached to stripped Decemet's membrane fragments.

IPE Immunohistochemistry

Confirmation of epithelial origin was achieved by immunohistochemistry using a monoclonal anti-pan cytokeratin antibody. Cells were counterstained with hematoxylin. Cultured human fibroblasts were tested as a comparative control and IPE cells without primary antibody served as a negative.

Transduction of IPE Cells

Human and rat IPE cells were cultured in 6-well plates with F-12 media supplemented with 20% FBS. Cells were transduced with 6×10^9 particles of eGFP virus. Confluent eGFP transduced IPE cells were monitored by inverted fluorescence microscopy (Leica DMIRB) for an extended time period to evaluate long-term lentiviral driven transgene expression. Fluorescent images were taken at day 7, day 40, day 100, day 150 (human IPE cells), and day 7, day 90 (rat IPE cells). At day 100, one well of human IPE cells was split into three wells to observe eGFP expression after passage.

Transduction and Analysis of RPE, CF, and Corneal Cell Lines

Cells were cultured in 6-well plates one day prior to the addition of the lentivirus. 1×10^9 particles of eGFP lentivirus was added to each of the wells and incubated with at 37°C, 5% CO_2 for 24 hours. Media was exchanged and the cells were grown in normal growth medium for 3 to 4 days. The transduced cells were collected after trypsinization and fixed in PBS containing 1% paraformaldehyde. The percentage of cells expressing eGFP in the different cell lines was determined by fluorescent-activated cell sorting (FACS). A time course study using RPE, CSC, and CF cells was also performed to evaluate long-term lentiviral driven expression. Cells were seeded into several 6-well plates and transduced with 1×10^9 particles of eGFP lentivirus, then continued in culture with normal growth medium for a period of 3 months. Expression was monitored in the same fashion as the IPE cells.

Rat Aortic Ring Assay

Four 8- to 10-week-old male Sprague Dawley rats were sacrificed, and the thoracic aortas were excised and placed into ice-cold EBM media (Cambrex Inc) supplemented with gentamicin and 10% FBS. The adipose was removed and the aortas were flushed to remove coagulated blood. Ten to 20 1-mm rings were cut from each aorta and were washed with fresh EBM eight times. The rings were separated and placed into a six-well plate containing EGM-1 media (Cambrex) that had been supplemented with gentamicin. Wells were inoculated with either 1×10^9 particles of sKDR virus, 1×10^9 particles of sNRP-1 virus, both (5×10^8 particles each of sNRP-11 and sKDR virus), or 1×10^9 particles of eGFP virus. Aortas were incubated overnight at 37°C 5% CO_2. The following day the aortas were embedded into 500 μL of Matrigel and covered with 2 mL of EGM-1 media containing 9000 pg/mL of human VEGF. The assay was incubated for 5 days and the aortas were photographed by digital photo microscopy. The images were analyzed by a blinded observer and graded on a scale of 1 to 5. The grades were averaged by dose and by group.

Production of AGE

Ribose induced AGE proteins were generated with 50 mg/mL of recombinant human serum albumin (GTC Biotherapeutics Co) and bovine serum albumin (Fraction V, Sigma Inc) incubated under sterile conditions with 0.5 M D-ribose for a week at 37°C in the presence of antibiotics and phenylmethylsulfonyl fluoride (PMSF). Control nonglycated serum albumin was incubated in the same conditions except contained no reducing sugar. Unincorporated sugars and low molecular weight reactants were removed by using PD-10 column chromatography (Pierce) and dialysis against PBS (pH 7.4). The final protein concentration was determined using a Bradford assay. To confirm AGE formation, the molecular weights of each protein were analyzed for a band shift using a silver stained PAGE gel. Human microvascular endothelial cells (HMVECs, Cascade Biologics Inc) were maintained in medium 131, supplemented with growth supplement. AGE treatment was carried out in 131 medium containing 5% FBS without growth supplement. Trypsinized microvascular endothelial cells were plated in 6-well culture plates at a density of 2×10^4 and were treated with 50, 100, 200, and 500 μg/mL of AGE for 4 days. Viable cells were counted using a hemocytometer.

Cell Proliferation Assay

MVECs were plated at density of 2×10^3 cells/well in 96 well plates, and incubated overnight at 37°C in 0.1 mL of 131 media with growth supplement. Cells were transduced with 1×10^9 particles of recombinant lentiviral vector containing soluble RAGE and/or full length RAGE and incubated for 2 days. Culture media was exchanged and 100 μg/mL of ribose-induced AGE was added and further incubated for 2 days. After incubation, cell proliferation was assessed by the 3-(4,5-dimethylthiazol-2-yl)-2,5-diphenyl-2H-tetrazolium bromide (MTT) method.

Measurement of VEGF Protein

MVECs were incubated with 100 μg/mL of ribose-induced AGE for 24 hours. Media was collected and VEGF concentrations were assessed with a VEGF ELISA kit (R&D Systems Inc).

IN VIVO EXPERIMENTATION, RABBIT MODELS

Corneal Pocket Assay

General anesthesia was induced in rabbits by masking with Isoflourane (2 L/min) and oxygen (1.5 L/min). One drop of proparacaine was placed in the fornix for topical anesthesia. The eye was prepped and draped in a sterile fashion. A lid speculum was placed in the eye. A 2.8-mm microkeratome was used to enter the corneal stroma at the 12-o'clock position. This intrastromal incision was developed into an 8-mm-diameter intrastromal pocket via a combination of blunt and sharp dissection with McPherson forceps and an iris sweep. The 12-o'clock incision was widened to 6 mm with Vannas scissors. A 4×4-mm Amersham hybridization nylon mesh (Amersham Inc) was saturated with 1×10^9 particles Endo:Ang lentivirus and was inserted into the preformed pocket (Figure 3).
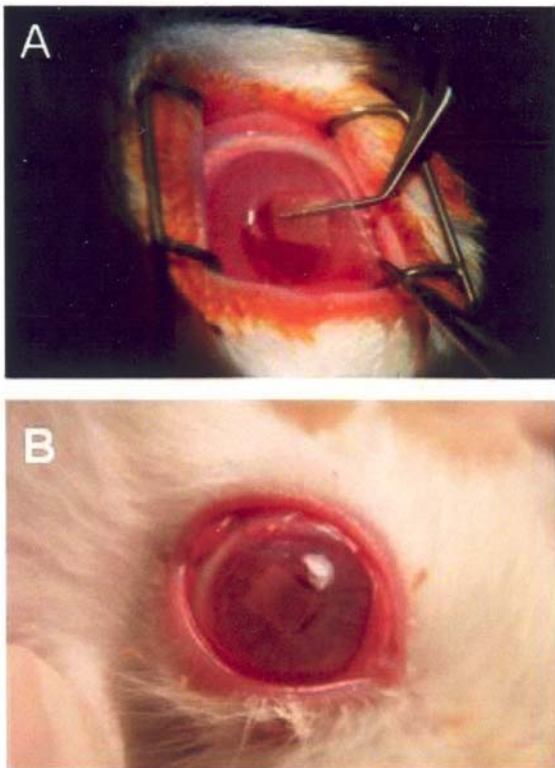

FIGURE 3

Stromal pocket assay. A, Insertion of viral saturated nylon mesh into the stroma of a rabbit's cornea. B, Cornea 24 hours after the procedure. Immunogenic response was not observed.

Subconjuntival injections of 0.1 cc of Enrofloxacin and Kenalog (40mg/cc) were given.   Postoperatively, all rabbits received 0.2 cc of Buprenex, topical atropine, and tobramycin.   On the first postoperative day, under topical anesthesia, the nylon mesh was removed. One week after removal of the virus-impregnated mesh, under topical anesthesia, either two 6-0 silk sutures were placed in the corneal stroma, 5 mm from the superior limbus, or a 6-mm-diameter disk of #3 Whatman filter paper soaked in 20 mL of 1 M NaOH was placed on each cornea for 1 minute (Figure 4). The eye was then rinsed with 0.2 cc of BSS. All animals were treated postoperatively with topical atropine and tobramycin.
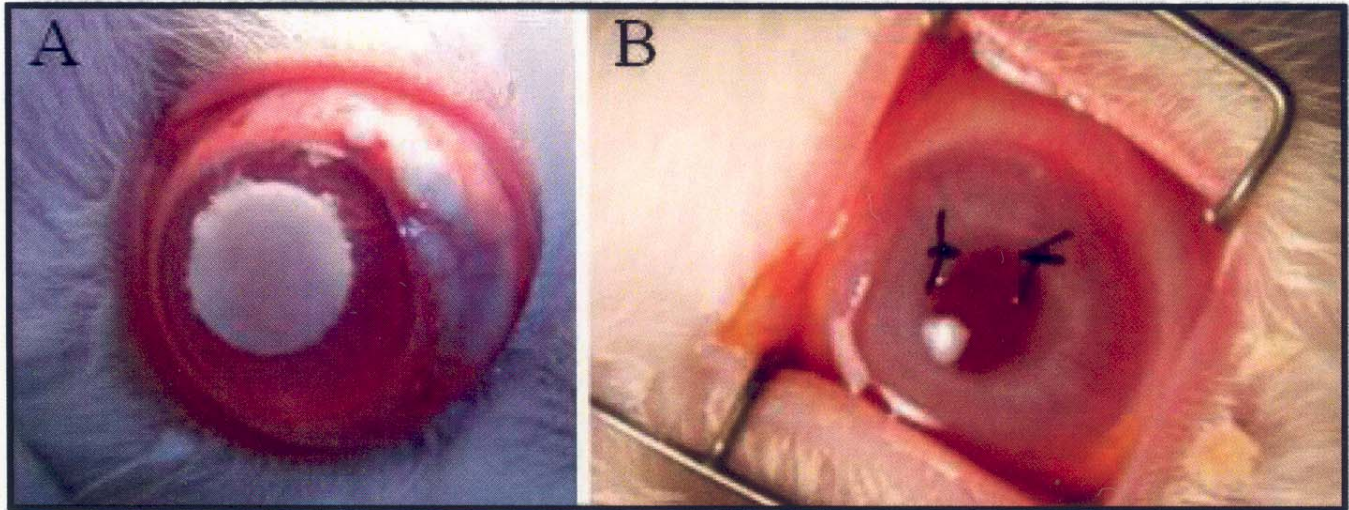
FIGURE 4

Corneal angiogenesis induction. Two methods used to initiate angiogenesis in the cornea. A,
Alkali burn by NaOH-soaked Whatman paper. B, Intrastromal silk-suture stimulus.

PKP Model

Sixteen 7-mm trephined donor corneas were obtained from eight New Zealand white rabbits. Each button was harvested in a sterile surgical fashion and placed in 2 mL of Optisol-GS (corneal storage media containing chondroitin sulfate dextran media supplemented with gentamicin [100 µg/mL] and streptomycin sulfate [200 µg/mL]) (Chiron Inc). The media was spiked with 50 µL (1.5×10^9 particles) of Endo: Kringle5 lentivirus, 50 µl (1×10^8 particles) of eGFP lentivirus, or 50 µL PBS. These buttons were incubated for 18 hours at 37°C. General anesthesia was induced by mask-administration of isoflorane. A paracentesis was created, and heparin and viscoelastic were instilled into the anterior chamber. A Hessburg-Barron 7-mm trephine was used to remove the host corneal button. A 7-mm-trephined corneal button previously treated with Endo: Kringle5, eGFP, or PBS was rinsed in BSS and grafted with 16 interrupted 7-0 nylon sutures.   0 .1 cc subconjuntival injections of Baytril (23 mg/cc) and Kenalog (40 mg/cc) were given. Postoperatively, all animals received a single dose of topical atropine (1%) and a single dose of Carprofen at 2.5 mg/kg SQ, as well as tobramycin, 1 drop twice a day for 5 days, and Buprenex at 0.1 mg/kg SQ as necessary.   No topical steroid drops were given postoperatively.

Tenon's Ex vivo Transduction and Transplantation

New Zealand white rabbit Tenon's fibroblasts were harvested by direct dissection. The Tenon's tissue was trypsinized into a monocell suspension by incubation with 0.25% trypsin and pipetting the cells through a 5-mL pipette. The cells were plated into six-well culture plates and allowed to grow to confluency in wells containing DMEM supplemented with 20% FBS. 1×10^8 particles of eGFP lentivirus, 1×10^8 particles of each of sNRP-1 and sKDR lentivirus and 1×10^8 particles of sNRP and sKDR (50:50 ratio) were introduced into separate wells. Tenon's cells transduced with eGFP were examined under fluorescent microscope to confirm transduction and transgene expression. Transduced Tenon's cells were trypsinized with 0.25% trypsin and made into a monocell suspension by mixing with PBS. Four different Tenon's suspensions were generated: naive Tenon's, Tenon's transduced with sNRP-1 and sKDR lentivirus, respectively, and Tenon's transduced with both (sNRP-1 and sKDR). Cells were counted and concentrated equally (approximately 85,000 cells per 0.5 mL of suspension). The eyes of 12 New Zealand white rabbits received subconjunctival injections of 0.5 mL of Tenon's suspension or PBS control into the inferior fornix of each eye with a 25-gauge needle. Injections included: three eyes with PBS, four eyes with naive Tenon's, four eyes with eGFP Tenon's, three eyes with sKDR Tenon's, five eyes with sNRP-1 Tenon's, and five eyes with "Both." On day 4 after subconjunctival injections, 6-0 silk sutures were placed 2.5 mm away from the limbal edge at the 6- and 12-o'clock positions of each eye.

Subconjunctival Lentiviral Injections

Anesthesia was induced in rabbits by a subcutaneous injection of a ketamine (0.5 mg/kg). Eyes were prepped and draped in a sterile fashion, and lid speculum was placed in the operative eye. Subconjuntival injections of 1×10^8 or 5×10^8 particles of Endo: Kringle5 lentivirus or PBS control were given in the inferior conjunctiva centered on 6 o'clock. Postoperatively, all rabbits received 0.2 cc of Buprenex (0.3 mg/cc) SQ bid for 1 day, and tobramycin bid for 4 days. Two weeks after the injection of the lentivirus or control, rabbits underwent induction of anesthesia with ketamine and surgical prep as previously mentioned. One 6-0 silk suture was placed in the corneal stroma 5 mm from the superior limbus, and one from the inferior limbus. All animals were received the above-mentioned postoperative care.

Intravitreal and Subretinal Viral Injections

Intravitreal injection: General anesthesia was induced in New Zealand Red rabbits by masking with isoflurane (2 L/min) and oxygen (1.5 L/min). One drop of proparacaine was placed in the fornix for topical anesthesia. Both eyes of the rabbit were dilated by a mixture of 1% Cyclogyl, 2.5% phenylephrine, 0.5% tropicamide, and 0.5% scopolamine. One eye was prepped in a sterile fashion and lid speculum was placed. A 30-gauge needle was use to inject 1×10^9 particles of either sNRP-1 or sKDR lentivirus (50 μL) into the vitreous through a point 3 mm posterior to the limbus.

Subretinal injection: Anesthesia administration and field preparation were accomplished as above. A small conjunctival peritomy was made with Wescott scissors, and an MVR blade was used to create a sclerotomy. Using an operating microscope and fundus contact lens, a subretinal injection of lentivirus (1×10^9 particles of either sNRP-1 or sKDR lentivirus in 50 μL) with a 39-gauge cannula was performed. 7.0 Vicryl was used to close the sclerotomy, and the conjunctiva was reapproximated.

Postoperatively, all rabbits received 0.2 cc of Buprenex (0.3 mg/cc) SQ bid for one day, topical atropine, a drop of Ocuflox, a drop of prednisolone, and a ½-inch ribbon of erythromycin ointment. On the first postoperative day, all rabbits were checked for infection and comfort.

Intravitreal VEGF Administration

Sedation was induced in New Zealand Red rabbits with a subcutaneous 1.5-cc injection of a mixture of ketamine, acepromazine, and xyalazine (5:1.5:1). Both eyes were prepped in a sterile fashion, and a lid speculum was placed. A 30-gauge needle was used to inject 0.625 μg of human VEGF (PanVera) 3 mm posterior to the limbus. Postoperatively, all rabbits received a drop of Ocuflox, a drop of prednisolone, and a ½-inch ribbon of erythromycin ointment. VEGF injections of 0.625 μg were performed 8, 11, and 18 days after viral injection. On days 23, 33, and 39 post viral injections, the VEGF dose was increased to 1.25 μg.

IN VIVO EXPERIMENTATION, PRIMATE MODELS

Subretinal Injection

Cynomolgus primates (*Macaca fascicularis*, Sierra Biomedical Inc) were anesthetized by intramuscular injection of a mixture containing ketamine hydrochloride (20 mg/mL) and acepromazine maleate (0.125 mg/mL). Pupils were dilated, eyes were topically sterilized, and proparacaine hydrochloride was used as topical anesthesia. A 20-gauge microvitreoretinal blade was used to create a sclerotomy 1.5 mm posterior to the corneal limbus. A 39-gauge rigid cannula (Synergetics Inc) was employed to deliver 0.3 mL of either 1X (1×10^8 particles) of K1-5 lentivirus, 10X (1×10^9 particles) of K1-5 lentivirus, 1×10^8 particles eGFP lentivirus, or PBS beneath the macula through a small, self-sealing retinotomy.

Laser Burn

Subretinal neovascularization (SRN) was induced in the macula, between the temporal vascular arcades, using an argon green laser (532 nm, Iridex Inc) via a stabilized slit-lamp delivery system. Nine spots in a 3×3 grid were created with single spot irradiation at 200 to 250 mW for 0.1s with a diameter of 75 μm. The presence of a small focal intravitreal hemorrhage suggested the penetration of Bruch's membrane. Six months after the initial laser treatment, additional laser was applied to unique macular sites to test for a long-term antiangiogenic effect.

QUANTITATION OF NEOVASCULARIZATION AND ANALYSIS

Fluorescein Angiography (FA)

Fundus angiography and photography was performed by dilating both eyes using a mixture of 1% Cyclogel, 2.5% phenylephrine, 0.5% tropicamide, and 0.5% scopolamine. Sedation was induced in rabbits with a subcutaneous 1.5-cc injection of a mixture of ketamine, acepromazine, and xyalazine (5:1.5:1). A RetCam (Massie Research Labs Inc) was used to image the posterior pole. Following color photography, 0.5 cc of fluorescein was injected into an ear vein with a 27-gauge needle. Images were obtained as early and late images looking for retinal vascular leakage by standard techniques.

Corneal Angiogenesis Grading

Grading was achieved by slit-lamp examinations post corneal insult (ie, corneal suture or alkali burn). Measurements of neovascularization were made with a portable slit lamp by a single observer. Serial photographs of the cornea were taken. Vessel growth onto the clear cornea was noted in millimeters and number of clock hours (using area = $3.14 \times$ radius in mm^2). Neovascularization was quantified by calculating the area of vessel growth.

Retinal Edema Grading

Grading was performed using FAs read by two independent masked observers. Edema was defined as none, mild, moderate, and severe. Mild was defined as early vessel change, but with minimal fluorescein extravesation. Moderate was defined as clear leakage with moderate vessel change. Severe was defined as significant leakage or neovascular changes of the optic nerve head. None, mild, moderate, and severe edema were defined as 0 to 3 for quantification purposes, respectively.

SRN Grading (Primate Model)

Fluorescein fundus photography was used to visualize the retinas of the primates every 2 weeks. Masked retinal specialists graded all photographs and angiographs. Grading was based upon a scale from 0 to 3 (0 = late staining around laser scar, 1 = early, limited hyperfluorescence with leakage, 2 = moderate leakage extending into the midphase of a 10-minute angiogram, 3 = persistent late leakage with large neovascular complex). After readministration of the laser-induced SRN, the masked observers cross-referenced the former fundus photographs in order to compare long-term and short-term K1-5 protection.

Primate Electroretinogram (ERG)

Multifocal ERGs were recorded using VERIS (version 4; EDI Inc) under general anesthesia (induction: 15 mg/kg IM ketamine; maintenance: 1.5% isoflurane). Pupils were fully dilated (≥7 mm) with 1% tropicamide and 2.5% phenylephrine (Alcon Laboratories Inc), and topical corneal anesthesia and lubrication were provided with 0.5% proparacaine (Alcon Laboratories Inc) and 1% methylcellulose, respectively. Custom-designed Burian-Allen contact lens electrodes were used for all ERG recordings (10-mm diameter, +3.00 diopter; Hansen Ophthalmics Inc); the corneal ring on the stimulated eye served as the active electrode, and the corneal ring of the unstimulated (patched) contralateral eye served as the reference electrode. Both electrodes were referenced to a subcutaneous ground electrode placed in the thigh. Electrode impedance was accepted if <5 kΩ. Residual refractive error was measured by retinoscopy for the test distance (25 cm) and corrected to the nearest 0.50 diopter. The multifocal ERG stimulus was presented on a 21-inch monochrome monitor with a 75-Hz refresh rate. Prior to the actual recording session, an initial set of brief recordings (2 minutes each) was used to center foveal responses within the response array and to position the "blind spot" responses appropriately. Fixation stability was monitored by direct visual inspection of both the eye and the online recording (ie, baseline stability). On rare occasions, small drifting eye movements and/or twitch-like partial blink artifacts (indicating insufficient depth of anesthesia) required re-recording of particular ERG segments. The multifocal ERG stimulus was a slowed local luminance flicker of 103 unscaled hexagonal elements subtending a total field size of ~55 degrees (see Figure 2). The luminance of each hexagon was independently modulated between dark (1 cd/m^2) and light (200 cd/m^2) according to a predetermined pseudorandom, binary m-sequence with a base-interval of 106.7 msec, providing local contrasts of ~99%. Stimulus luminances were measured using a calibrated spot photometer (SpectraScan PR-650, Photo Research Inc). Each recording was ~8 minutes in length (usually obtained in eight 60-sec segments). Signals were amplified (gain = 100,000), band-pass filtered (10 to 300 Hz; with an additional 60 Hz line filter), sampled at 1.2 kHz (ie, sampling interval = 0.83 msec), and digitally stored for subsequent off-line analyses.

Pathology

Histopathology was used to examine tissue for anatomical changes that may have occurred during experimental procedures. Briefly, eyes were enucleated, grossly examined, and placed into either formalin or 4% paraformaldehyde. Fixed tissue was then dehydrated and paraffin embedded. Sections were cut to a thickness of 5 μm using a microkeratome fitted with a diamond blade. Slides were prepared and stained with hematoxylin and eosin.

IN VIVO MOLECULAR ANALYSIS

RNA Isolation and RT-PCR

Eyes were enucleated and bisected and the target tissue (ie, retina or cornea) was dissected and placed into RNA LATER storage solution (Ambion Inc). RNA was isolated, and RT-PCR was performed in a similar fashion as stated above.

RESULTS

LENTIVIRAL PRODUCTION

The angiostatic cDNAs: Endo: Ang, Mig:IP10, sKDR, Timp-1, sNRP-1, K1-5, Endo: Kringle5, and sRAGE were all successfully cloned into the lentiviral vector pHR-CMV-ires-eGFP. The plasmids were sequenced verified and used to produce replication deficient lentiviral particles. Titers were estimated by P24 GAG ELISA and averaged 1×10^7 particles per μL. All lentiviral preparations were verified to be infective and capable of producing transgene mRNA by RT-PCR and/or by demonstrating green fluorescence by visualization using an inverted fluorescent microscope.

IN VITRO STUDIES OF TRANSDUCTION

Time Course Studies

Ocular cell lines used in this study were either isolated by primary culture or obtained from the ATCC. Cells were studied for both transduction efficiency and transgene expression capabilities. IPE cells isolated from human and rat donor eyes displayed

characteristic spindle or polygonal shaped morphology. Both cell derivations tested positive for cytokeratin by immunohistochemistry, confirming epithelial origin. Control fibroblast cells were negative after employing the anti-cytokeratin antibody, demonstrating cellular specificity (Figure 5).

Cells were examined by fluorescent microscopy 7 days post viral transduction and exhibited strong green fluorescence. At day 40, 80% to 90% of cells appeared to express the green fluorescent protein. By day 100, a marked decrease in fluorescence was noted and cultures at day 140 were observed as having a green fluorescent appearance in approximately 40% of total cells. Subcultures of transduced human IPE at day 100 grew well, but the fluorescent phenotype was limited to 20% of cells (Figure 6).

Over 90% of RPE cells and 55% of CF cells were positive for eGFP expression 72 hours post viral incubation when incubated with the same viral titer. The duration of stable expression of eGFP from transduced cells was determined over a period of 3 months. The initial number of RPE cells expressing eGFP after 7 days reached 95%. This level of expression was stable and persisted for 90 days. Similar stable expression was obtained for 65% of transduced CF cells (Figures 7 and 8).
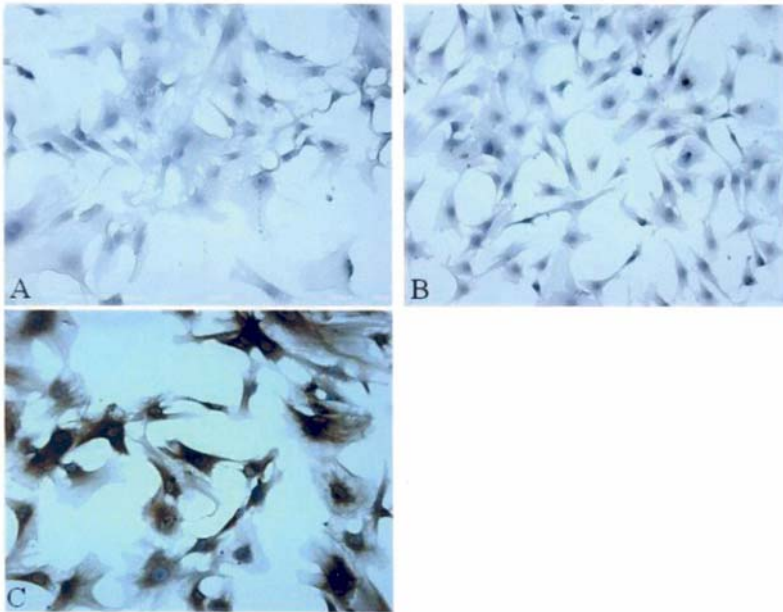
FIGURE 5

Iris pigment epithelial (IPE) immunohistochemistry. A, Human IPE primary culture. B, Rat IPE primary culture. C, Human IPE cells staining positive using the antibody anticytokeratin, a specific marker for epithelial cells. All cells are shown at 40× magnification.
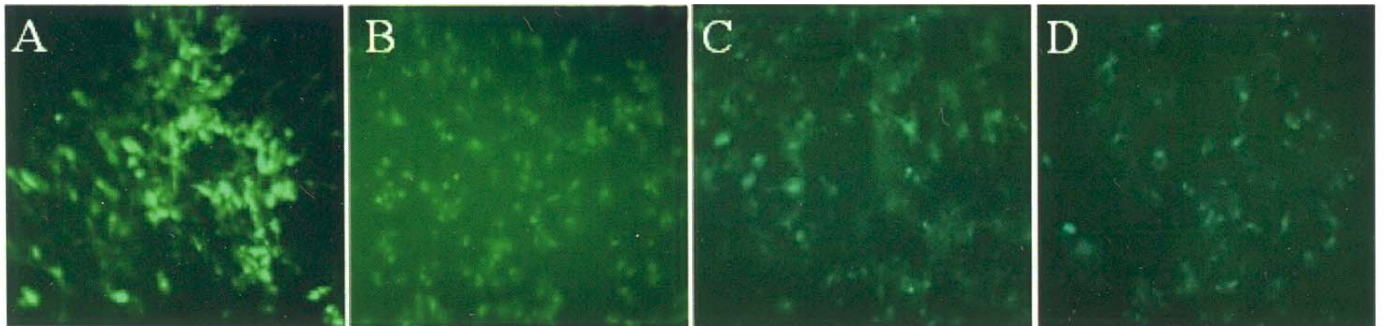
FIGURE 6

Iris pigment epithelial (IPE) transgene expression. Expression of eGFP in transduced human IPE cells was photodocumented from IPE cells observed at day 7 (A), day 40 (B), day 100 (C), and day 140 (D).

Cells of the cornea (ie, epithelial, stromal keratocytes, and endothelial) when plated separately displayed over 90% transduction efficiency after the first week post viral incubation. eGFP expression was robust and persistent for at least 90 post-transfection days. Whole cornea culture and incubation with eGFP lentivirus demonstrated that the epithelial and endothelial layers were transduced with high efficiency, whereas intracorneal stromal keratocytes (not exposed to viral media) were devoid of eGFP expression; this pattern was observed for the full 60 days of experimental observation (Figure 9).

All cell lines used in this study maintained normal in vitro morphology. Exposure to and transduction by lentiviral particles and eGFP expression were not associated with obvious cellular toxicity and/or cell death.
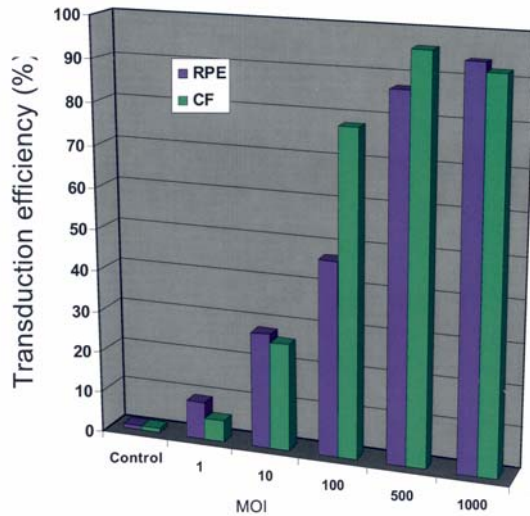
FIGURE 7

Transduction efficiency in retinal pigment epithelial (RPE) and choroidal fibroblast (CF) cells. Both cells demonstrated increased transduction efficiency with increased multiplicity of infection (MOI). Expression reached greater than 90% in cells when 500 to 1,000 viral particles per cell were administered.
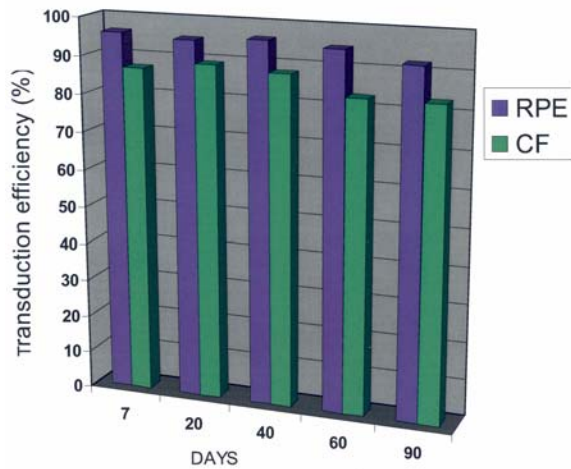
FIGURE 8

Temporal transgene expression in retinal pigment epithelial (RPE) and choroidal fibroblast (CF) cells. Both cell lines demonstrated persistent transgene expression for the full 90 days. RPE cells were capable of higher levels of expression compared to CF cells.
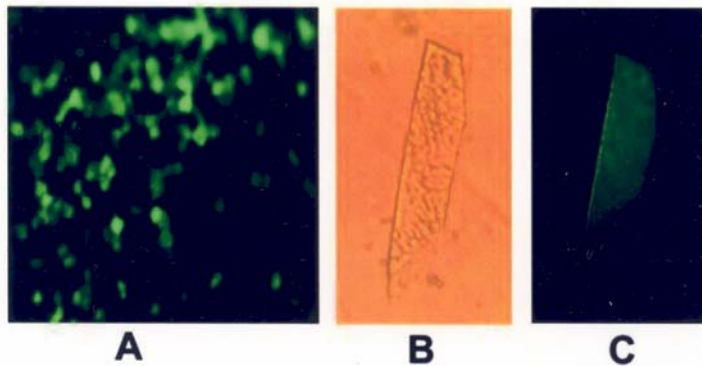
FIGURE 9

Corneal transduction via eGFP lentivirus. Corneas were observed 3 days post-transduction; endothelial cells were positive for eGFP expression (A). Stripped Descemet's membrane with attached endothelial layer observed in white light (B) and fluorescent light (C). Reprinted, with permission, from Nature Publishing Group. *Gene Therapy* 2000;7(3):196-200.

Aortic Ring Assay

Rat aortic rings were incubated in the presence or absence of virus for a total of 5 days, after which vessel growth was observed. Within dose groups (ie, hVEGF treated), growth appeared sporadic with no trend toward a dose-growth relationship. Growth between sets of rings transduced and control rings did show variation. Naive, eGFP, and the sNRP-1 rings exhibited approximately equivalent vessel growth, ranging 3 to 4 on the grading scale. Rings transduced with sKDR had fewer neovascular tufts, and overall vessel length was shorter. Rings transduced with both sNRP-1and sKDR displayed slightly reduced vessel formation compared to sKDR alone and were nearly a full grade lower than controls and rings infected with sNRP-1alone (Figure 10). There was no significant difference observed between experimental groups within this assay (Figure 11).
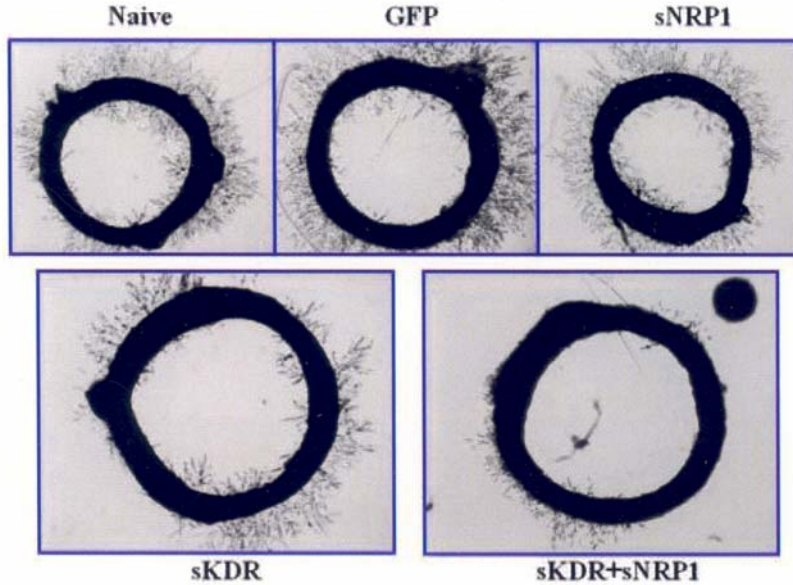
FIGURE 10

Rat aortic ring assay. Rings were evaluated for vessel growth and density. Rings transduced with both sNRP-1 and sKDR lentiviral vectors demonstrated the least amount of vessel development; however, statistical significance was not achieved.
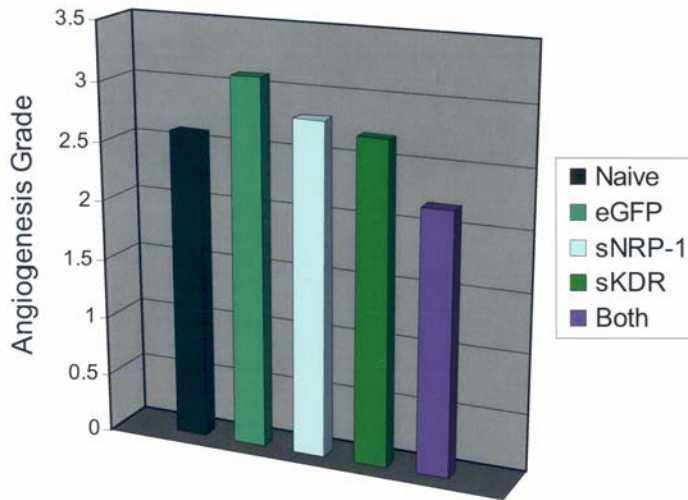

FIGURE 11

Aortic ring inhibition. Evaluation of angiogenesis from aortic rings was graded by a blinded observer, on a scale of 0 to 4. Aortas that were transduced with both sNRP-1 and sKDR lentiviral particles displayed the highest amount of vascular regression; however, this was not statistically significant.

Cell Proliferation Assay Using Advanced Glycosylation End Products

During advanced glycation, the amine groups of albumin were modified by the sugar ribose, resulting in a modified albumin molecular weight; this was confirmed by a denaturing SDS-PAGE analysis. Ribose-induced AGE increased the molecular weight of albumin by about 9.2 kD when compared with the unmodified serum albumin control. AGE-modified albumin significantly reduced in vitro cell proliferation when 100 μg/mL of AGE serum was used. This was observed by manual cell counting MVECs treated with AGE compared to PBS and control serum albumin (Figure12).

The MTT assay demonstrated a trend of growth inhibition by sRAGE lentivirus compared to controls, although this trend was statistically not significant. Analysis of VEGF by ELISA was performed to determine whether the sRAGE lentivirus was capable of inhibiting downstream VEGF production in MVECs. The result of this experiment revealed no significant difference in VEGF levels between any of the experimental groups (Figure 13).
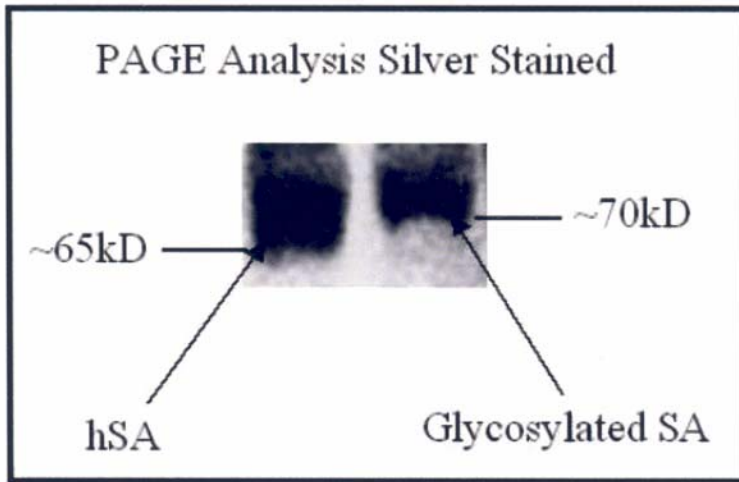
FIGURE 12

Ribose-induced AGE formation was confirmed by SDS-PAGE. After incubation, the molecular weight of human serum albumin (hSA) had shifted approximately 9.2 kD by the addition of the glycosylation end products.
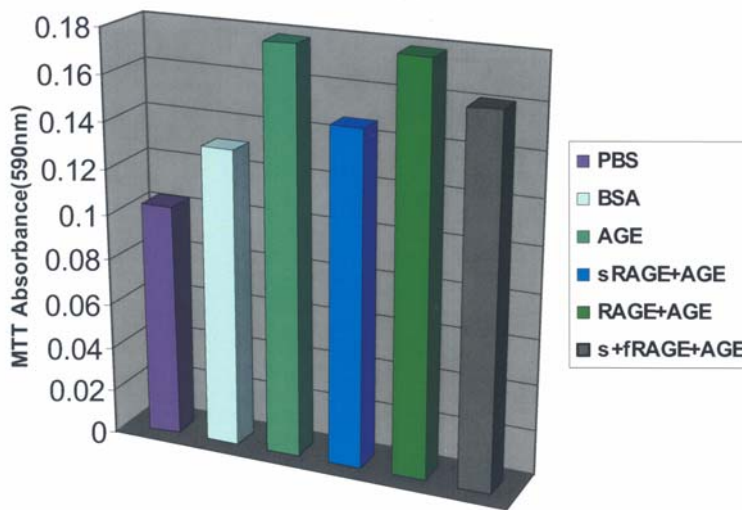
FIGURE 13

Effects of soluble and full-length receptors to advanced glycosylation end products (AGE). Cell proliferation was assessed by MTT analysis. sRAGE displayed a nonsignificant trend of inhibition seen in microvascular endothelial cells compared to cells that had received AGE-modified serum albumin alone.

IN VIVO STUDIES OF TRANSDUCTION, RABBIT MODELS

Corneal Pocket Assay

SKDR. Measurement of neovascularization (NV) was assessed 3, 5, 7, and 10 days after the delivery of lentivirus and angiogenic induction via interstromal suture. Less NV was observed in corneas, which had received sKDR, compared to controls (Figures 14 and 15). Examination of hematoxylin-eosin stained histology slides revealed that control eye sections contained a large numbers of blood vessels and basophilic infiltrates. Tissue that had been incubated with sKDR appeared less edematous and demonstrated a marked reduction of inflammation. Blood vessels were either not present or small and nontortuous in sKDR samples (Figure 16).

FIGURE 14

Stromal suture induction of corneal angiogenesis. Lentiviral particles were delivered via the corneal pocket method; these photos represent corneas 7 days after angiogenesis was stimulated with corneal sutures. The sKDR cornea is relatively clear and free of invasive blood vessels. The PBS eye displays a significant angiogenic and immune response.
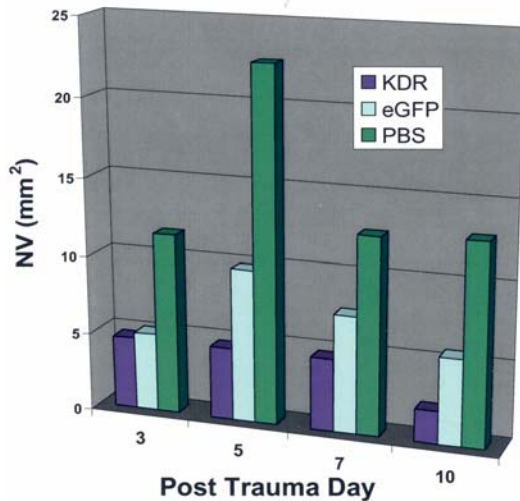
FIGURE 15

sKDR corneal angiogenesis inhibition. The sKDR treated corneas were associated with significantly less neovascularization ($P < .05$) than corneas treated with PBS at days 5, 7, and 10.

MIG:IP10. Visual examination of eyes 10 days post insult with NaOH displayed a marked difference in controls vs *Mig:IP10* treated eyes (Figure 17). Analysis of NV showed a treatment-associated reduction as follows: a 58% reduction in NV at day 3, 68% reduction at day 5, 74% reduction at day 7, and 55% reduction at day 10 in treated vs eGFP lentivirus delivered control eyes. A similar trend was observed when treated eyes were compared to PBS delivered (Figure 18). Hematoxylin-eosin histology slides were made from eyes in all groups 11 days postinsult. Sections from control eyes contained a large number of blood vessels and inflammatory infiltrates; whereas *Mig:IP10* treated corneas appeared devoid of both vessel growth and immune response (Figure 19). Despite biologic effect, transgene expression by RT-PCR was not unequivocally demonstrable.

ENDO:ANG. Eyes were observed at 3, 5, 7, and 10 days postinsult via intrastromal sutures. Control eyes developed significant corneal edema, and in several cases the cornea became completely opacified (Figure 20). There was less NV observed in eyes treated with *Endo:Ang* lentivirus during the early stages of the neovascular response; however, this trend reversed after 7 days. At no time was a statistically significant difference between treated animals and controls noted (Figure 21). Histological examination of corneas treated with either PBS or eGFP lentivirus displayed a significant immune response evidenced by the large number of infiltrates in the stroma of these corneas. Treated eyes did stain positive for immune cells but contained less than control eyes. Blood vessels were not present in corneas treated with the *Endo:Ang* lentivirus, although it was noted that the epithelia layer of treated corneas did appear more edematous than normal or naïve tissue (Figure 22).
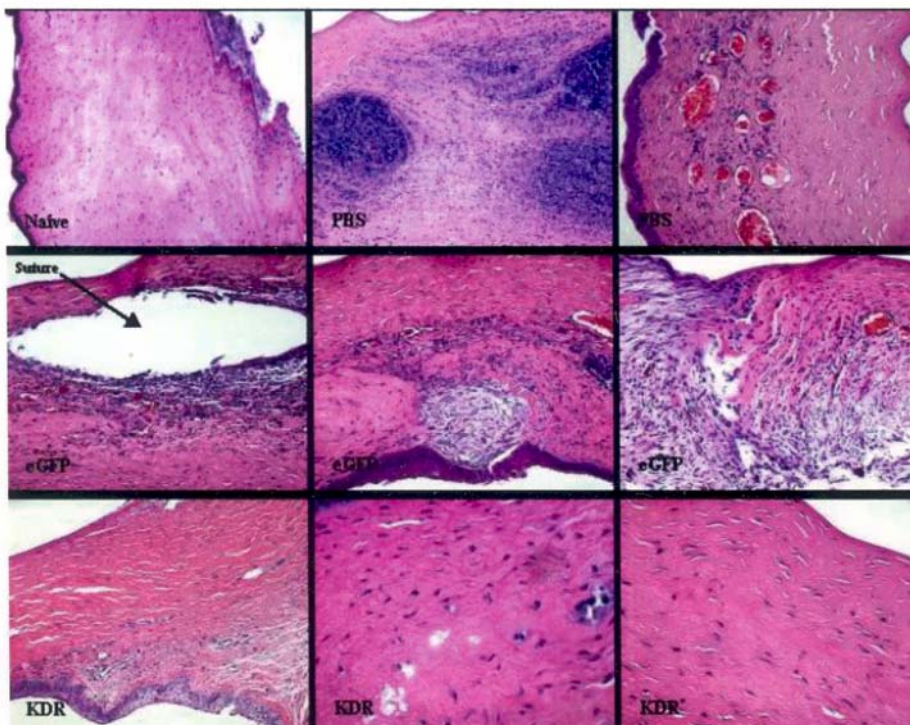

FIGURE 16

Histopathology of sKDR lentivirus treated corneas. The top three images represent corneal histopathology of naïve or PBS control animals, the middle three images are from lentiviral-eGFP controls, and the bottom three images are from lentiviral-KDR treated animals. PBS and eGFP samples contain many aberrant blood vessels and basophilic infiltrates. The sKDR cornea appears healthy and similar to the naïve specimen.
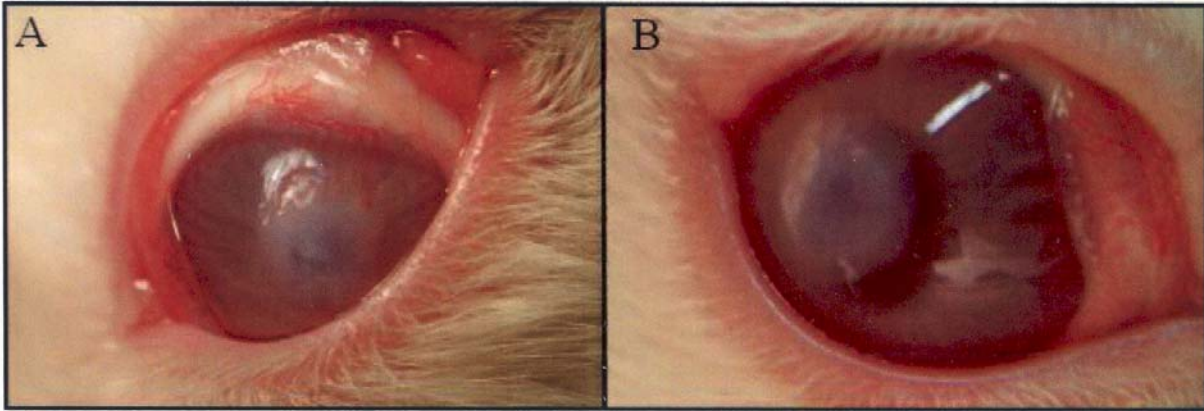
FIGURE 17

Lentiviral MIG:IP10 antiangiogenic effect. Corneas were photographed 10 days post NaOH induction of angiogenesis. Corneas treated with eGFP lentivirus (A) displayed more development of blood vessels compared to MIG:IP10 lentiviral treated (B). Central corneal haziness is a result of the NaOH burn.

TIMP1. Measurement of neovascularization was assessed at days 3, 5, 7, and 10 after angiogenic induction with NaOH burn between rabbit corneas that had received *Timp1* lentivirus, eGFP lentivirus, or PBS. No significant difference was observed in the extent of neovascularization between any of the experimental groups (Figure 23). Transgene expression as measured by RT-PCR was not unequivocally demonstrable in all samples tested (Figure 24). Hematoxylin-eosin histology of corneal sections from *Timp1* lentiviral and control eyes displayed moderate blood vessel development with less seen in the angiostatic treated group; also noted was the decrease in inflammation seen in Timp1 specimens compared to controls (Figure 25).

PKP Model

Corneal neovascularization associated with corneal transplant rejection was significantly lower ($P < .05$) in lentiviral *Endo: Kringle5* transplanted eyes on postoperative days 5, 12, 14, 16, 18, 24, 28, and 36 compared to corneal buttons treated with eGFP lentivirus or PBS (Figure 26). All PBS and all lentiviral eGFP treated corneas exhibited neovascular arborization into the graft bed. No vessel growth into the graft was observed in corneas treated with *Endo: Kringle5* lentivirus. It was demonstrated that three of three PBS and two of three eGFP lentiviral treated corneas exhibited corneal opacification and subsequent graft failure, whereas all 10 *Endo: Kringle5* lentivirus treated grafts remained clear and free of rejection by postoperative day 39 (Figure 27).

The five grafts tested by RT-PCR for the presence of fusion gene transcripts were positive on postoperative days 30 and 40. All control and naive eyes were negative for the fusion gene by RT-PCR (Figure 28).
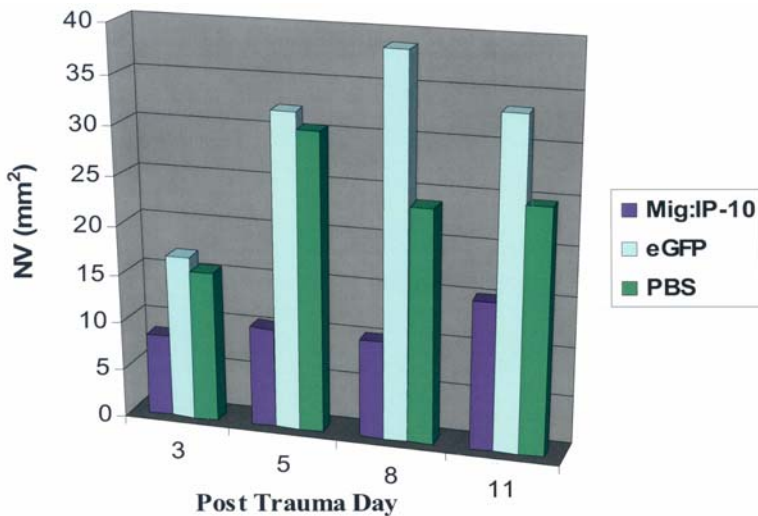
FIGURE 18

MIG:IP10 corneal angiogenesis inhibition. Neovascularization was significantly reduced (*P* < .05) at days 5 and 8 in animals treated with the MIG:IP10 fusion virus, compared with animals treated with PBS
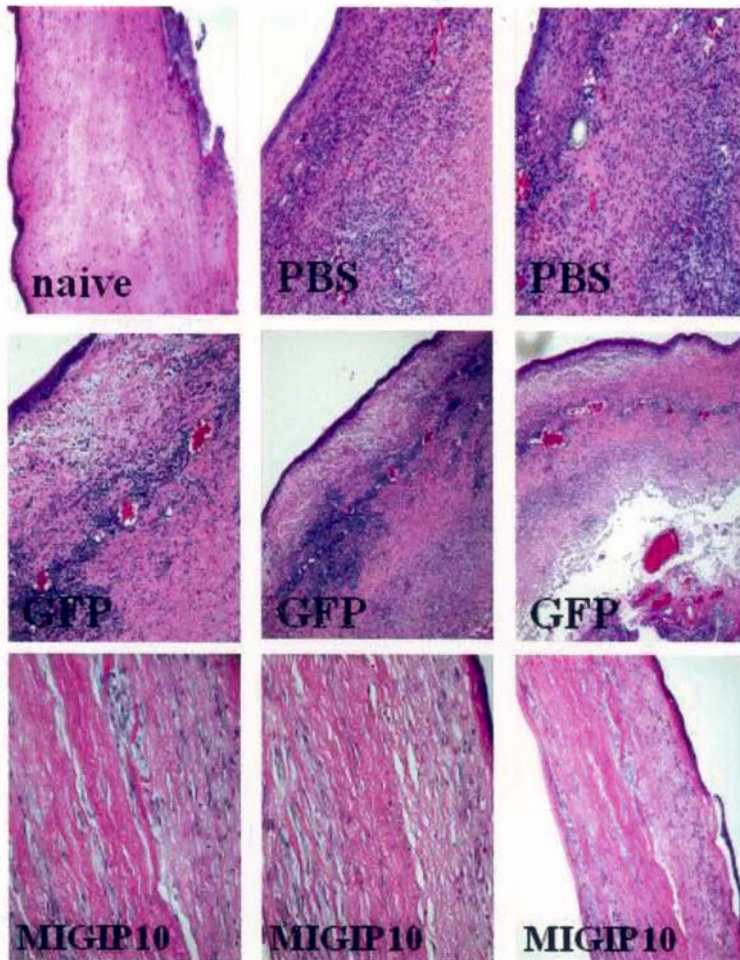
FIGURE 19

Histopathology of MIG:IP10 lentivirus treated corneas. The top three images represent corneal histopathology of naïve or PBS control animals, the middle three images are from lentiviral-eGFP controls, and the bottom three images are from lentiviral-MIG:IP10 treated animals. PBS and eGFP samples contain many aberrant blood vessels and basophilic infiltrates. The MIG:IP10 cornea appears healthy and similar to the naive specimen.
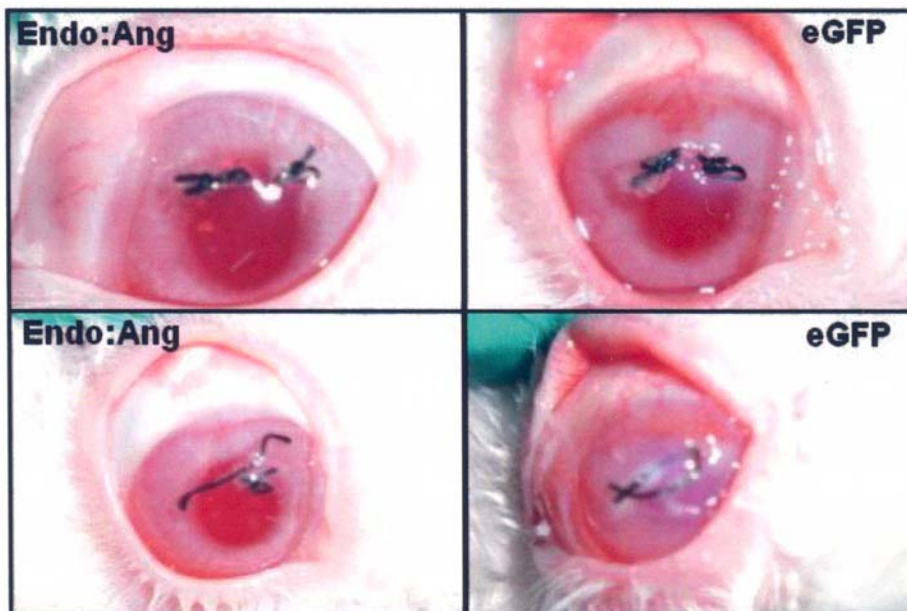
FIGURE 20

Suture induction of corneal angiogenesis. Lentiviral particles were delivered via the corneal pocket method; these photos represent corneas 10 days after angiogenesis was stimulated with corneal sutures. The Endo:Ang cornea is relatively clear and free of invasive blood vessels. The eGFP eye displays a significant angiogenic and immune response, including extensive corneal edema and opacity.

Histopathology of the grafts revealed thicker, more edematous corneas in the controls when compared to the *Endo: Kringle5* treated corneas. Analysis of serial sections revealed more neovascularization and basophilic inflammatory infiltrates in controls than in *Endo: Kringle5* treated or nonoperated eyes. Study of a retained suture site by histology in an *Endo: Kringle5* cornea was void of inflammatory cells, usually the location of increased immune response (Figure 29).
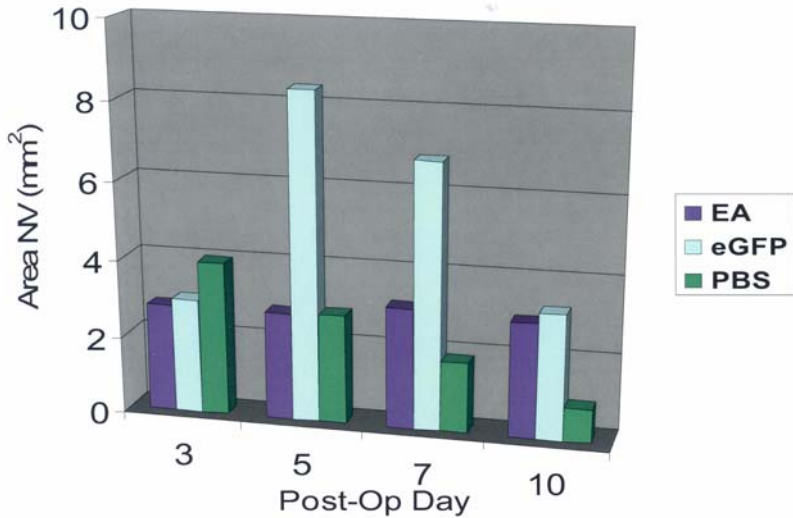
FIGURE 21

Endo:Ang corneal angiogenesis inhibition. No significant inhibition of neovascularization was observed in animals treated with Endo:Ang fusion lentiviral particles compared with controls.

Ex vivo Tenon's Model

Tenon's tissue demonstrated successful ex vivo transduction using eGFP lentivirus by fluorescent microscopy examination, and cells transduced with either sNRP-1, sKDR, or both (sNRP-1 and sKDR) were confirmed for transgene expression by RT-PCR (Figure 30). The area of neovascularization in eyes injected with PBS, naive Tenon's cells, Tenon's transduced with eGFP lentivirus, *sNRP-1* lentivirus, *sKDR* lentivirus, or both (*sNRP-1* and *sKDR*) lentiviruses were examined after angiogenic stimulation by suture placement at day 4, 8, 12, and 17 (Figure 31). Significant inhibition was observed at a single time point (day 12) in eyes injected with cells transduced by both *sNRP-1* and *sKDR* lentivirus. There appeared to be a trend for less neovascularization in eyes injected with *sNRP-1* only compared to both (*sNRP-1* and *sKDR*) lentiviral transduced Tenon's cells, although this difference was not significant. Corneal neovascularization of PBS controls and eyes injected with Tenon's cells that had been transduced with both (*sNRP-1* and *sKDR*) lentiviruses suggested only a minor difference on day 8 and day 12 post suture induction (Figure 32).

Histopathology of the corneas showed stromal neovascularization and inflammatory infiltrates in all corneas tested. Compared to all groups, the *sKDR* lentiviral transduced Tenon's group displayed the lowest amount of stromal blood vessels invasion (Figure 33).

VEGF Retinal Edema Model

Retinal edema was documented with RetCam fluorescein angiograms and was graded by a masked ophthalmologist following serial injections of VEGF in the vitreous cavity of treated and control rabbits (Figure 34). After four intravitreal VEGF injections (the first three with 0.625 μg, the fourth with 1.25 μg), control eyes evidenced significant retinal vascular leakage compared to the angiostatic gene treated groups. Following a fifth VEGF injection, statistically significant less retina edema was seen in eyes that received either *sKDR*, *sNRP-1*, or both compared to the control eyes that received PBS (Figure 35). Further injections of VEGF induced an increased amount of vessel leakage and retinal edema in all eyes with less edema seen in the angiostatic treated groups compared to controls. Whereas significant differences were noted between treated and control animals, no difference was noted between animals that received angiostatic virus into the vitreous cavity or the subretinal space.
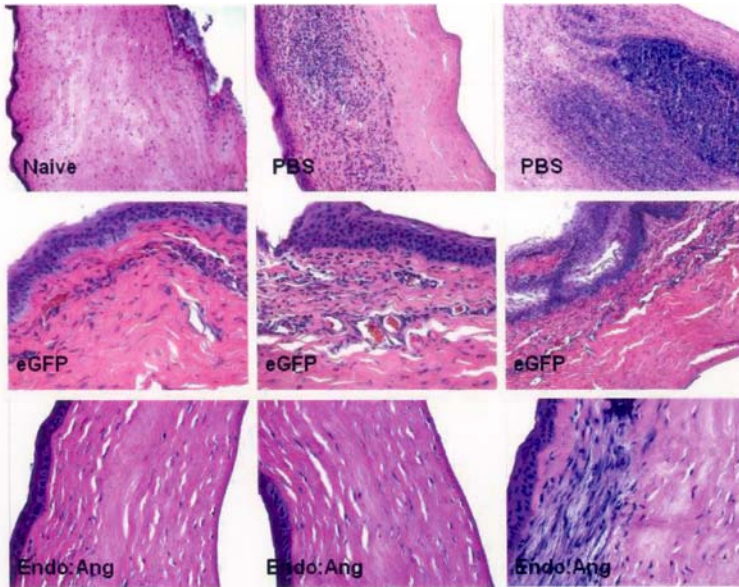
FIGURE 22

Histopathology of Endo:Ang lentivirus treated corneas. The top three images represent corneal histopathology of naïve or PBS control animals, the middle three images are from lentiviral-eGFP controls, and the bottom three images are from lentiviral-Endo:Ang treated animals. Vessel development is lower in all samples compared to similar experiments. Both the eGFP and Endo:Ang samples display significant corneal edema mainly associated with the superficial stromal and epithelial layers
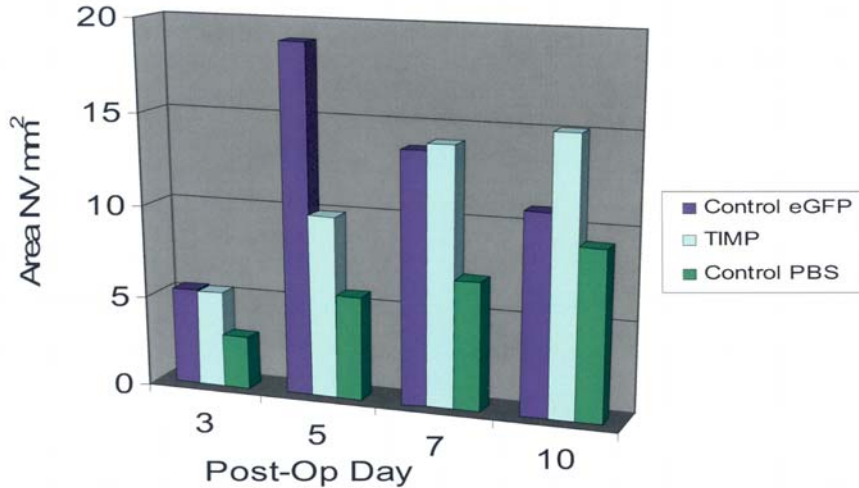
FIGURE 23

Timp1 corneal angiogenesis inhibition. No significant inhibition of neovascularization was observed in animals treated with Timp-1 lentiviral particles compared with controls.

IN VIVO STUDIES OF TRANSDUCTION, PRIMATE MODEL

Evidence of transgene expression of the *Kringle1-5* gene by RT-PCR in vivo after subretinal injection at 1 week and 6 weeks was demonstrated. Two weeks following the subretinal injection, eyes were treated with high-energy grid laser in the macula to stimulate the development of SRN (Figure 36). The laser presumably induced breaks in Bruch's membrane, which allowed the growth of new choroidal blood vessels through the RPE and into the subretinal space.

Viral particles delivered to the subretinal space are able to infect RPE cells and photoreceptor cells. Subretinal lentiviral transgene expression was confirmed by eGFP visualization 6 months after the initial injection, confirming that viral infection was contained within this area (Figure 37). In addition, the K1-5 gene used in this study was linked at the 5′ end to a secretion signal sequence adapted from the human interleukin-2 gene. This 20 amino acid secretion peptide will permit the expressed K1-5 protein to be exported out into the surrounding subretinal space, and possibly into the vitreous. The secreted K1-5 protein is in the ideal environment for targeting choroidal blood vessels that penetrate through Bruch's membrane into the subretinal space.
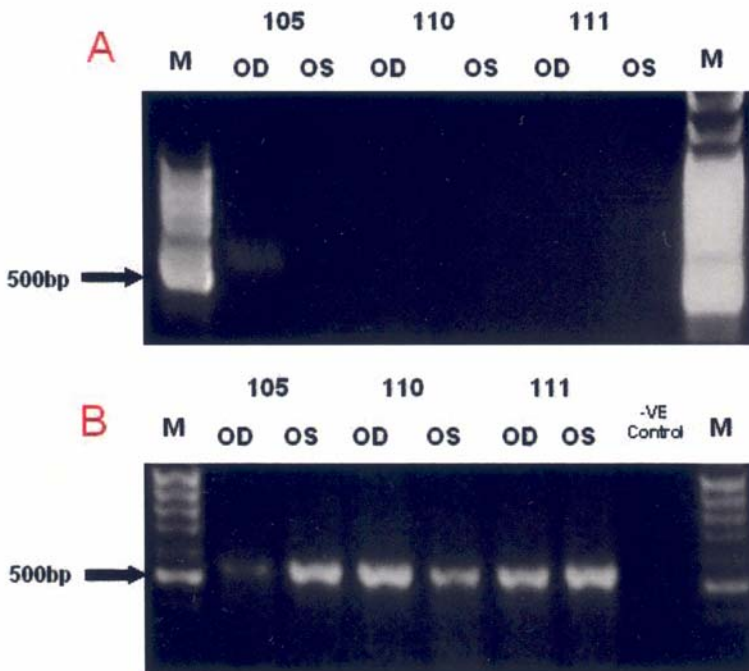

FIGURE 24

Timp-1 transgene expression. RT-PCR results from three subjects treated with Timp-1 lentivirus. Lentiviral Timp-1 was delivered to the right eyes of all animals; left eyes served as negative controls. A, Timp-1 message was present at low levels in one of three samples. B, Beta actin was used to demonstrate RNA level and quality.
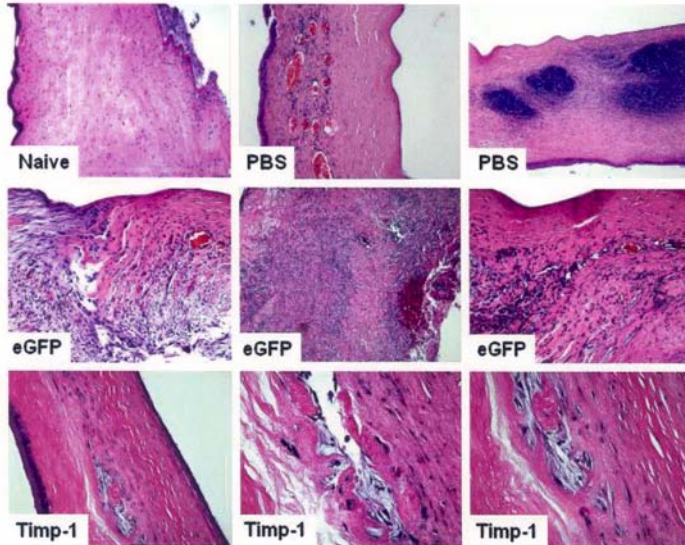
FIGURE 25

Histopathology of Timp-1 lentivirus treated corneas. The top three images represent corneal histopathology of naïve or PBS control animals, the middle three images are from lentiviral-eGFP controls, and the bottom three images are from lentiviral-Timp-1 treated animals. Intense basophilic infiltration and blood vessel development can be seen in PBS samples. There were fewer blood vessels observed in eGFP and Timp-1 corneas, yet a statistically significant difference was not observed.

The extent of laser-associated leakage (a surrogate marker for subretinal neovascularization) was measured clinically by direct ophthalmoscopy and fluorescein angiography every 2 weeks during postlaser months 1 to 3, and every 4 weeks during postlaser months 4 to 6 (Figure 38). Photographs and angiograms were independently graded by two masked retina specialists on a scale of 0 to 3, with 3 considered the most severe leakage. A dramatic reduction in the size and severity of SRN in eyes treated with lentiviral vectors containing the K1-5 gene when compared to control eyes at the 6-month stage after the initial laser induction was observed (Figure 39). Significant difference was seen between controls for either concentration 1X ($P = .04$) or 10× ($P = 8.15 \times 10^{-6}$). Significant difference between K1-5 treated and eyes injected with control lentivirus ($P = .00027$) was also noted. No significant difference between the 1× and 10× concentration was observed. After 6 months of observation, the second laser treatment was performed to restimulate the development of SRN in all maculae, at sites distinct from the initial treatment site. Further FA data resulted in a marked reduction in SRN at month 10 time point with significant difference between 10× viral K1-5 treated eyes and contralateral controls ($P = .0006$) and sub-retinal injected controls ($P = .0017$). No difference was observed between contralateral controls and sub-retinal injected controls or between 1× and 10× K1-5 treated eyes (Figure 40).

Lentiviral subretinal injections did not perturb retinal function as evidenced by multifocal ERG analysis (Figure 41); neither the concentration of lentiviral vectors employed nor the method of delivery perturbed retinal function, suggesting that the vector and gene product were both nontoxic. The overall responses recorded from eyes that received a subretinal injection, whether with lentivirus or saline, were similar to those from the control eye for all animals. There was a trend for the group of eGFP eyes to have slightly smaller multifocal ERG response amplitudes and slightly longer implicit times, but there were no significant differences across study groups for either parameter.
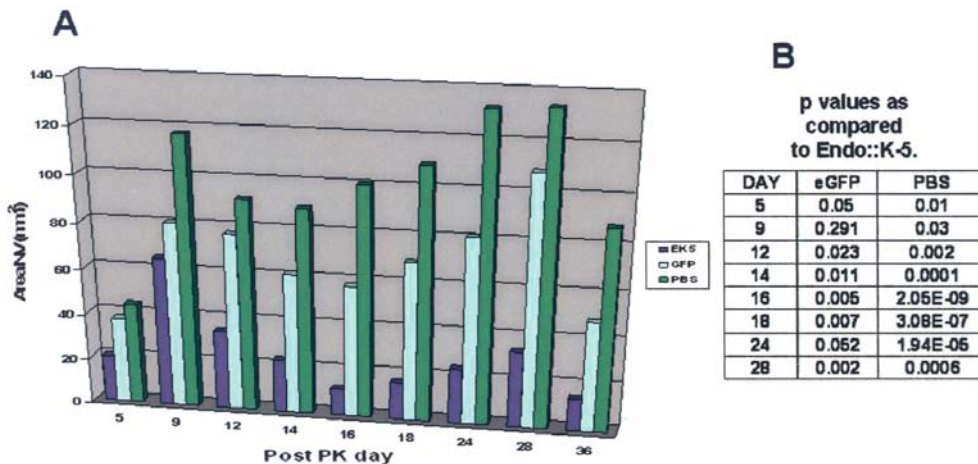
FIGURE 26

Endo:Kringle5 corneal angiogenesis inhibition. A, The average area of neovascularization in postoperative Endo: Kringle5 and control treated corneas is shown. Standard deviation is shown for each time point. B, Standard *t*-test using a one-tail distribution comparing Endo: Kringle5 to eGFP or to PBS. All time points are significant with the exception of eGFP at day 9.
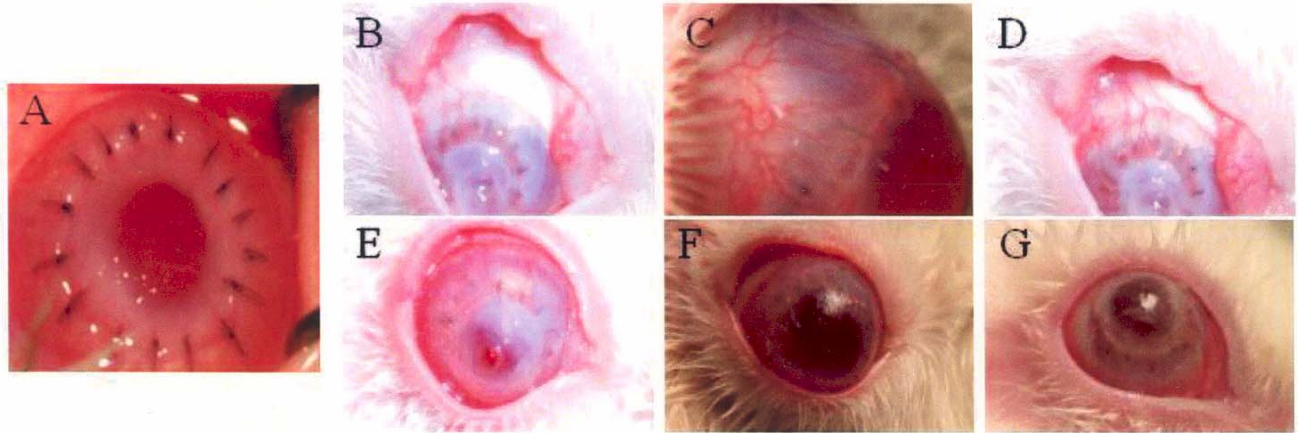
FIGURE 27

Post penetrating keratoplasty neovascularization and graft failure. Photographs of transplanted corneas that were pretreated with either virus or PBS. All transplanted corneas appeared healthy at day 0 (A). Corneas that received eGFP virus (B and C) were opaque and developed an extensive angiogenic response by day 14. PBS-treated corneas were opaque and vascularized at days 14 (D) and 40 (E). Endo: Kringle5 treated corneas remained clear and avascular at days 18 (F) and 40 (G). Reprinted, with permission, from the Association for Research in Vision and Ophthalmology. *Investigative Ophthalmology and Visual Science* 2003;44:1837-1842.
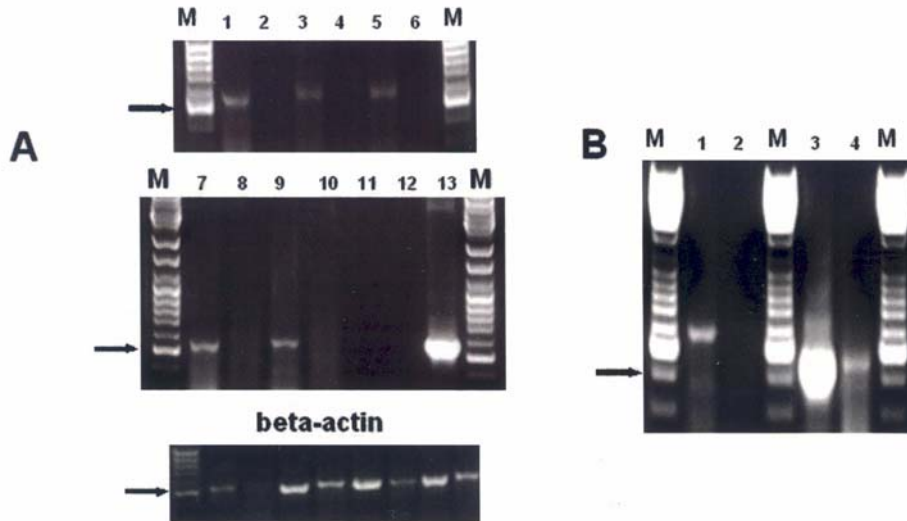
FIGURE 28

RT-PCR analysis of Endo: Kringle5 in transplanted corneal tissue. Right eyes were transplanted; left eyes served as nonoperative controls. A, At post-transplant day 30, RT-PCT was performed to detect transgene mRNA. Lanes 1, 3, 5, 7, and 9 correspond to Endo: Kringle5 mRNA positive samples. Lanes 2, 4, 6, 8, and 10 represent left eye negative controls. Lane 11 is an RT negative control, lane 12 is a PCR negative control, and lane 13 is an Endo: Kringle5 cDNA positive control. Beta-actin mRNA controls for lanes 1-8 is shown. B, At post-transplant day 40, RT-PCT was performed to detect transgene mRNA. Lane 1 demonstrates transgene transcription and lane 2 represents the negative contralateral control. Lanes 3 and 4 are beta-actin controls. Reprinted, with permission, from the Association for Research in Vision and Ophthalmology. *Investigative Ophthalmology and Visual Science* 2003;44:1837-1842.
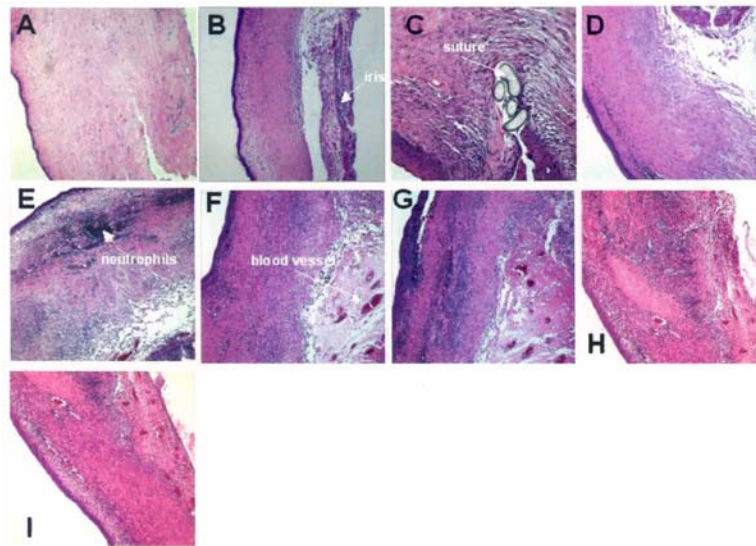
FIGURE 29

Histopathology of rabbit corneal transplants. A, Nonoperated naive cornea (normal). B, C, and D, Endo: Kringle5 treated buttons. Tissue is void of vessel proliferation, and only slightly elevated immune infiltrates (basophils) are present. E, F, and G, eGFP controls. There is an increased presence of immune cells, and a high number of blood vessel can be seen. H and I, PBS controls, similar to the eGFP sections with increased immune cell presence and vessels apparent in the stroma. Reprinted, with permission, from the Association for Research in Vision and Ophthalmology. *Investigative Ophthalmology and Visual Science* 2003;44:1837-1842.
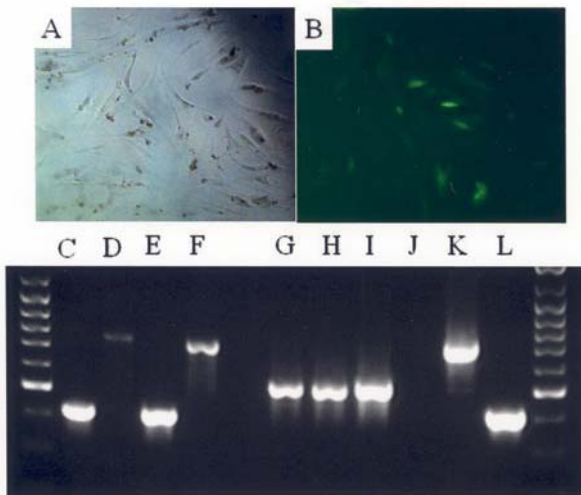

FIGURE 30

Demonstration of transgene expression in Tenon's cells. Microscopic examination of Tenon's fibroblast in white light (A) and fluorescent light (B). RT-PCR analysis of Tenon's cells (transduced ex vivo), expression of sNRP-1 alone (C), sKDR alone (D), both from the same Tenon's cells (E and F). Beta-actin was used to observe RNA quality and abundance (G through I). Negative and positive controls were also tested (J through L).
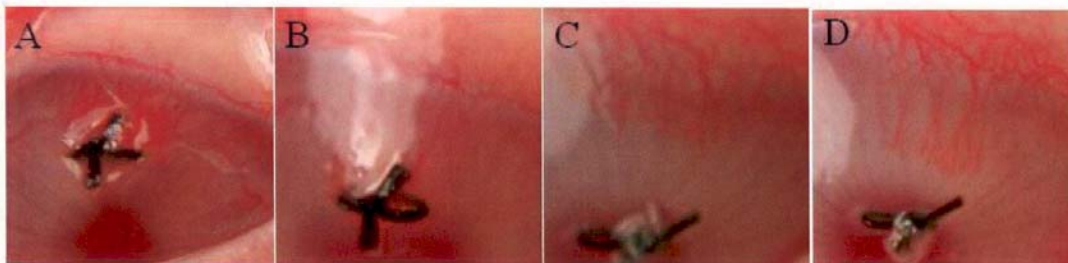

FIGURE 31

Corneal neovascularization in eyes transplanted with Tenon's cells transduced ex vivo. Angiogenesis induced by suture stimulus was observed in PBS treated (A and B) and in corneas treated with transplanted Tenon's cells transduced with both sNRP-1 and sKDR lentiviral particles (C and D). Photos were taken of the superior portion of the cornea; transplantation occurred in the inferior portion of the conjunctivae. There is little difference observed between treated and control groups.
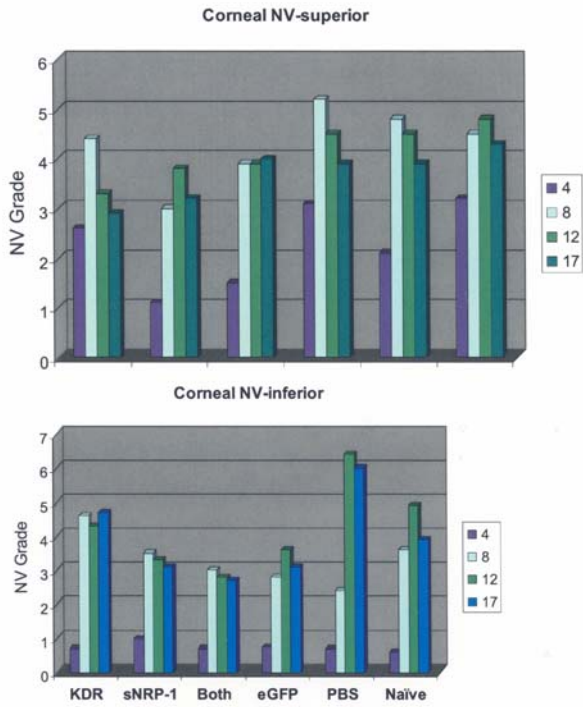
FIGURE 32

Superior and inferior corneal neovascularization. Inferior results show slightly more regression within the treatment groups as compared to the superior results. Considering cell transplants were delivered inferiorly an antiangiogenic effect is plausible, but differences are statistically insignificant. Data is presented at 4, 8, 12, and 17 posttransplantation days.
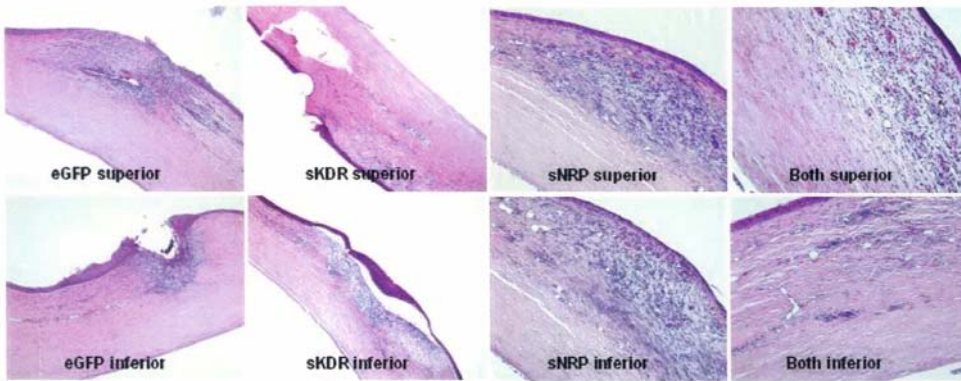
FIGURE 33

Histopathologic analysis of corneas from eyes transplanted with transduced Tenon's cells. Histopathology demonstrates little vessel or basophilic involvement in any of the experimental subjects.
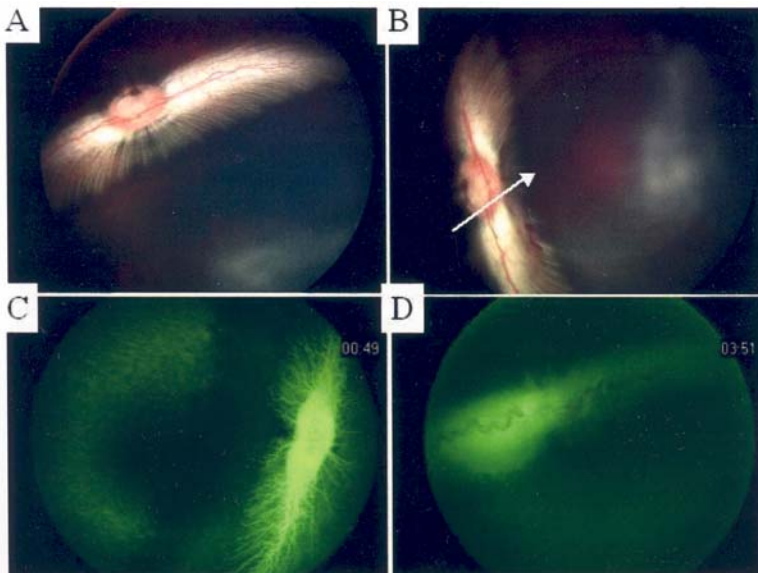
FIGURE 34

Rabbit lentiviral subretinal injection. Photograph of rabbit retina before (A) and after (B) subretinal injection. Fluorescein angiography (FA) of a retina 14 days postinjection of repeated VEGF administration; note vascular permeability (C) and tortuous blood vessels (D). Arrow indicates the location of the bleb created during injection.
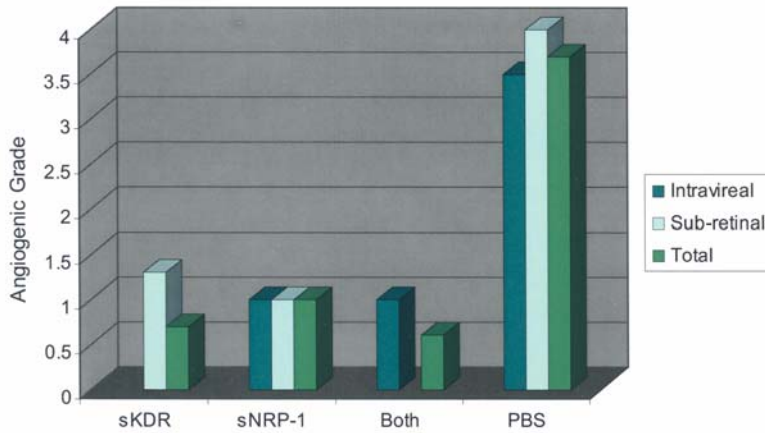
FIGURE 35

Grading for experimental groups. All groups displayed statistically insignificant trends toward angiogenic regression. There was no statistically significant difference observed between groups that were administered lentivirus by either intervitreous or subretinal injection.
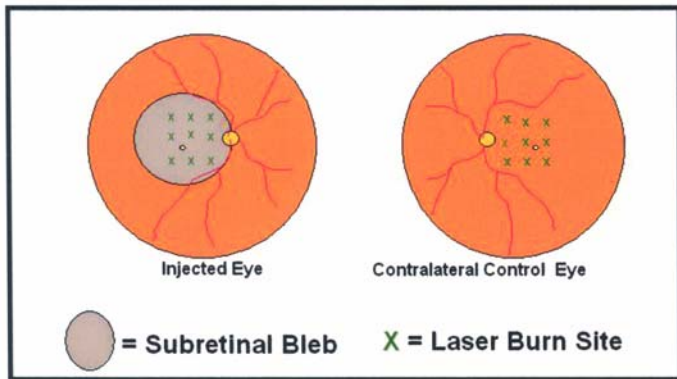

FIGURE 36

Schematic of primate subretinal neovascularization (SRN) experimental design. The right eye of each of 12 primates received a submacular injection of lentivirus containing either K1-5-ires-GFP or GFP only, or a sham injection with an equal volume of saline. The left eye served as a noninjection control. Subretinal injection results in the formation of a bleb underneath the retina (indicated). SRN was induced in the macula, in between the temporal vascular arcades, using an argon green laser in both eyes (laser burn sites indicated with an X).

FIGURE 37
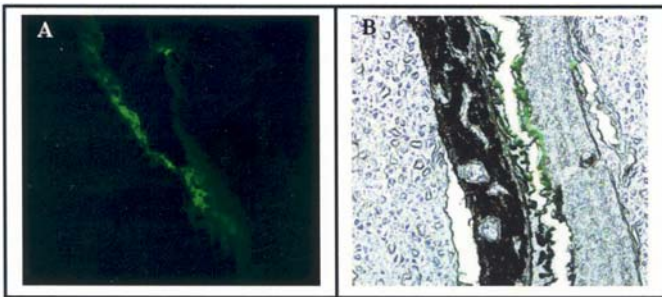
Subretinal eGFP expression. Viral particles delivered to the subretinal space infect retinal pigment epithelial cells and photoreceptor cells within the subretinal space. Lentiviral subretinal transduction was observed via GFP marker gene expression, confirming that viral infection is contained within the injection area. A, Fluorescent microscopy of a section through the retina of a subject that received a subretinal injection of lentiviral containing the GFP gene. B, Overlay of a light and fluorescent image of the same subretinal section.
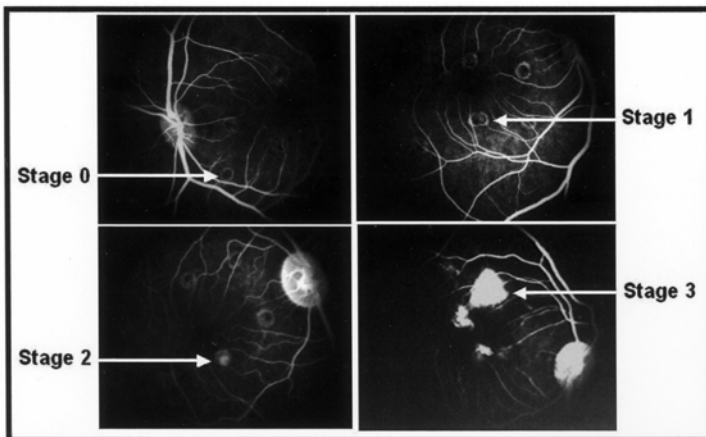
FIGURE 38

Primate fluorescein angiograms indicating different stages of subretinal neovascularization. Representative angiographs with stage 0, 1, 2, and 3 leakage as reviewed by two independent retinal specialists. 0 = late staining around laser scar; 1 = early, limited hyperfluorescence with leakage; 2 = moderate leakage extending into the midphase of a 10-minute angiogram; 3 = persistent late leakage with large neovascular complex.
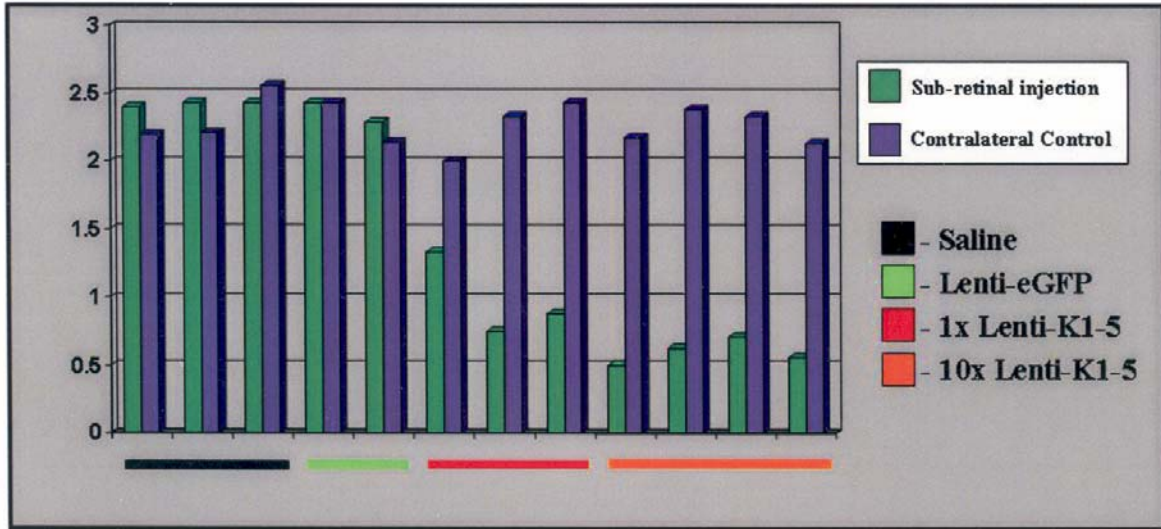
FIGURE 39

Primate subretinal neovascularization (SRN) data (6 months). Analysis of the fluorescein angiogram data revealed significant difference between eyes treated with K1-5 virus and control eyes at the 6-month stage. A total of 24 primate eyes were compared: five control subretinal injections, three saline (black underline) and two lentiviral GFP (green underline); seven lentiviral K1-5 subretinal injections (three 1× and four 10× concentration); and 12 noninjected contralateral controls. A statistically significant reduction in SRN was noted in K1-5 lentivirus treated eyes ($P < .05$).
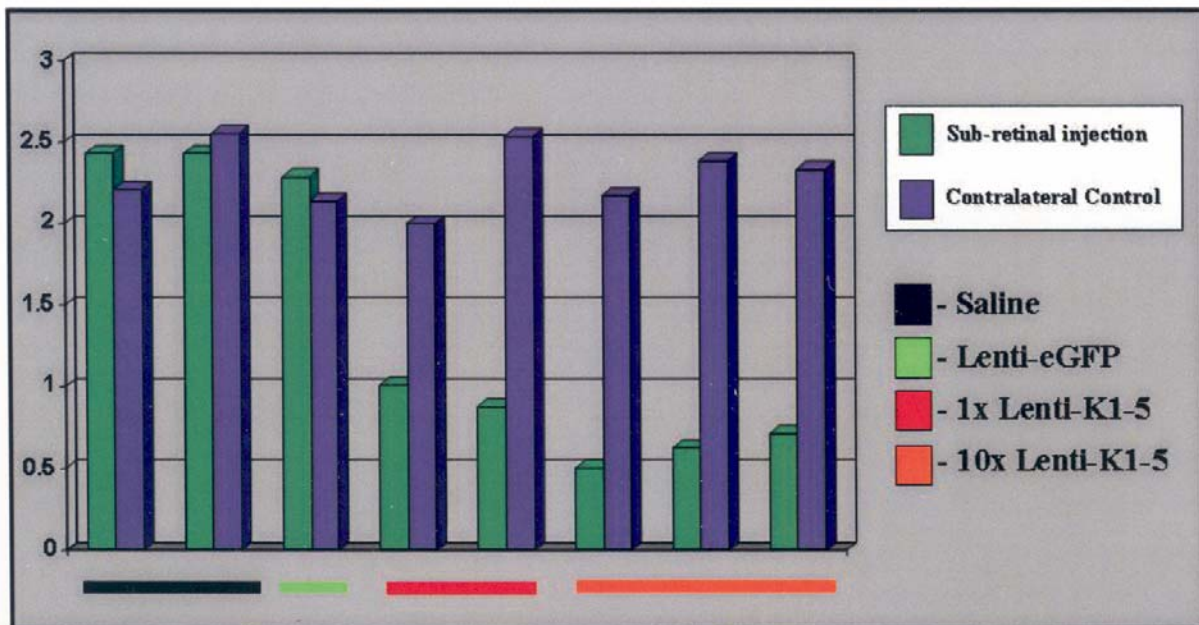
FIGURE 40

Persistent inhibition of subretinal neovascularization (SRN). After rechallenge by repeat laser to induce SRN again, the fluorescein angiogram data at the 10-month period revealed significant difference between 10× viral K1-5 treated eyes and contralateral controls ($P = .0006$) and subretinal injected control (GFP and saline) eyes ($P = .0017$). A total of 16 primate eyes were compared: three control subretinal injections, two saline (black underline) and one lentiviral GFP (green underline); five lentiviral K1-5 subretinal injections (two 1× and three 10× concentration); and eight noninjected contralateral controls.
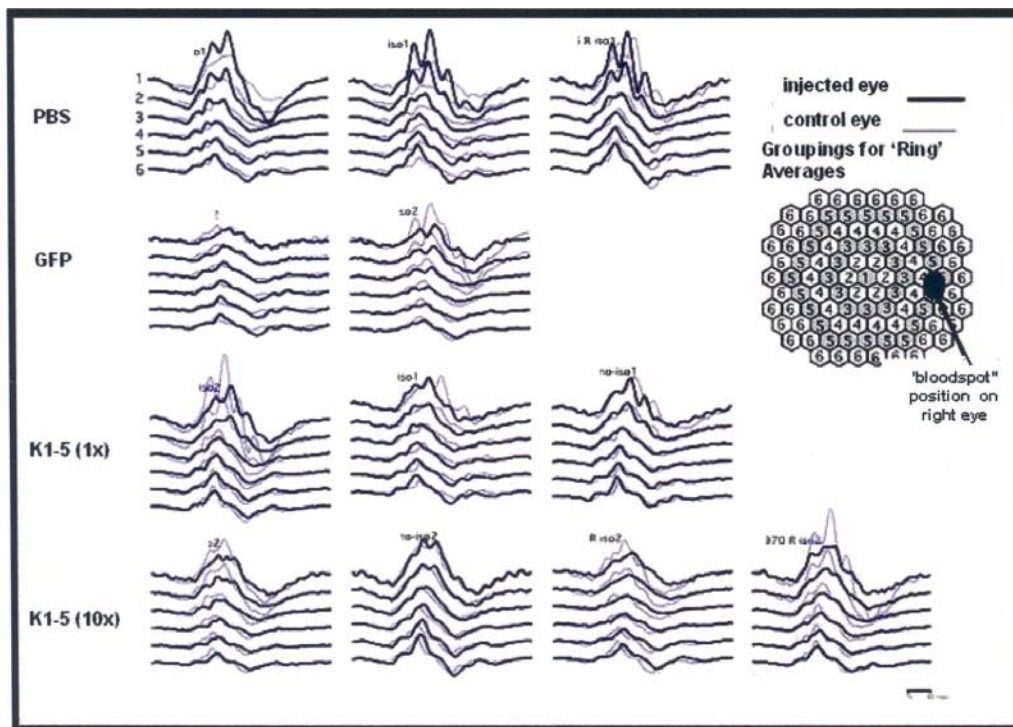
FIGURE 41

Multifocal electroretinogram (ERG) analysis. ERG indicates normal retinal function after injection of viral load. The responses from the injected eye (bold tracing) are similar to those from the control eye (gray tracing) for all animals. The subtle differences, such as reduction of the prominent second and third oscillatory potentials in central retinal responses, are related more to the duration of anesthesia due to the random order of eyes tested. The overall amplitudes of the initial negative and positive responses, analogous to the full-field ERG a-wave and b-wave, are similar between injected and control eyes.

DISCUSSION

IN VITRO STUDIES

The objective of these studies was to gauge the effectiveness an HIV-1 derived lentiviral vector in transferring genetic material (ie, eGFP) into a variety of target cells germane to human ocular disease in vitro and to analyze persistence of expression. The data presented demonstrate that lentiviral vectors are able to transfer and express transgenes in a variety of ocular cells.

An important issue to consider is transduction efficiency. These experiments demonstrated that lentiviral transduction efficiency varied considerably depending on the cell line tested. Corneal and RPE cells demonstrated 90% transduction efficiency and were most susceptible to lentiviral infection. The high degree of gene transfer to these particular cell lines suggests that therapeutic strategies that require persistent retinal or corneal gene expression may be possible. In contrast, IPE cells demonstrated strong early transgene expression, then a rapid loss of expression. Choroidal fibroblasts displayed persistent expression, but the percentage of transduced cells was lower than any of the other cell lines tested. Why only slightly more then half of CF cells were permissive is unclear

While long-term expression was observed in some cells, the results observed with IPE cells demonstrate variability between cells in the persistence of expression. It is unclear how this loss of function occurs on a molecular level. Possible explanations include variation in transduced cell survival, variation in the stability of integrated genetic material, and/or long-term gene silencing, perhaps via transgene methylation reactions. Although the CMV promoter was consistent for all cell types tested, it is possible that regulation of the promoter may differ between cell source and other cell-specific factors may be responsible.[34] The genomic site of integration of the vector may play a role in regulation of expression, and it is possible that location of integration, although thought to be random, may be predisposed depending on cell type.[35]

The potential to manipulate the expression of the integrated transgene using an inducible promoter system is worthy of intensive study. In many clinical situations (like DR or neovascular AMD), the proangiogenic stimulus is chronic and may persist some time after our current therapies. In these situations, it may be beneficial to have a persistent antiangiogenic stimulus, such as that favored by lentiviral transduction.

Transduction efficiency also varied depending on the growth stage and the concentration of virus used. The higher the concentration of virus added to cells (up to a MOI of 1:1000), the higher the transduction efficiency. This direct relationship seems to

be a logical correlation; it possible that multiple integration events increase overall expression patterns. No obvious signs of toxicity to the cells were observed, even when the highest concentrations were employed. This suggests that this vector may be applied successfully for clinical use without dose toxicity issues, although high titers may lead to other safety issues, such as excess integration leading to normal gene function knockout (ie, excess random integration).

It has been shown that AGE contribute to disease in patients with PDR[8]. Testing whether a soluble receptor to these end products is capable of inhibiting AGE-induced proliferation of cells that constitute blood vessels (MVECs) is an important question. However, the level of VEGF protein secreted from MVECs quantified by ELISA demonstrated that there was no difference in levels of VEGF protein between the AGE-induced group and controls. The AGE employed in this study was prepared using the sugar ribose. The result obtained may be explained by the fact that different reducing sugars may have disparate effects on VEGF gene expression; thus it is plausible that ribose AGE does not induce a strong stimulatory effect on VEGF expression.

Experiments analyzing the growth rates of AGE-treated MVECs suggest a trend toward inhibition of cell growth when the cells were pretreated with sRAGE lentivirus when compared to treatment with full-length RAGE lentivirus or naive cells that received AGE only. Cotransduction of MVECs with full-length RAGE and sRAGE lentivirus showed a slight inhibitory effect on MVEC cell division compared to the group treated with RAGE alone, which suggests that sRAGE may competitively inhibit RAGE-AGE-binding. The inhibitory effect of sRAGE was small and statistically insignificant. This lack of significant difference may reflect an ineffectiveness of sRAGE, incomplete competitive inhibition, or activation of other surrogate pathways separate to the RAGE signaling cascade. It would be interesting to study AGE products derived from other reducing sugars, such glucose, glycolaldehyde, and glyceraldehyde. Because diabetics produce a mixture of AGE adducts, testing combinations of various AGE products may more accurately mimic the clinical phenomenon of DR.

The rat aortic ring assay is an interesting model that attempts to bridge the gap between cellular-based assays and in vivo animal models. It was noted that coinfection of the rat aortic rings with lentivirus particles capable of expressing and secreting soluble VEGF receptors resulted in less vessel growth than in untreated rings when stimulated with VEGF protein. Interestingly, a strong correlation between VEGF dose to aortic vessel growth response was not observed. It is possible that the human isoform of VEGF used in these experiments is variably efficient at stimulating growth in rat aortic tissue slices in vitro. Previous studies have shown species specificity as a requirement for true functional analysis. An example of this is the use of endostatin in a rat aortic ring assay; the human isoform was ineffective as an inhibitor, yet when the murine isoform was used, inhibition was robust.[36]

IN VIVO RABBIT STUDIES

The rabbit models used for assessing antiangiogenic genes can be divided into two groups, corneal-based and retinal-based. Corneal angiogenesis was induced via three methods: the use of stromal sutures (represents a foreign body stimulus), corneal transplantation (PKP) and NaOH chemical burn (a traumatic injury model). To establish an efficient and reliable method of transferring lentiviral particles to the cornea or in the vicinity of the cornea to affect corneal angiogenesis, a variety of methods were tested. Transduction of stromal tissue was accomplished using a nylon mesh that had been soaked in lentiviral solution and then insertion of this mesh into an intrastromal pocket so as to achieve intrastromal transduction. In an alternative strategy, the cells on the peripheral edge of corneal buttons were transduced ex vivo prior to PKP, in the hope that cells from all three layers of the cornea would be capable of synthesizing an angiostatic protein after transplantation. Two additional methods were tested for remote delivery: the first involved direct injection of viral vector into the subconjunctival space, and the second was injection of ex vivo transduced cells derived from Tenon's capsule into the subconjunctival space. The latter approach offers the advantage of being able to confirm transduction of target cells prior to injection.

Stromal Suture Model

Lentivirus particles harboring *sKDR* gene delivered to the stroma were able to reduce neovascularization in a rabbit corneal angiogenesis model. Preliminary data suggest that this product is potentially useful for treating proliferative ocular disease. The Endo: Ang lentivirus delivered to the stroma was shown to be useful for studying the combined antiangiogenic properties of endostatin and angiostatin. The preliminary data from the rabbit model of corneal neovascularization shows less neovascularization in corneas transduced by Endo: Ang lentivirus when compared with controls. It would seem that intrastromal delivery of a vector producing an antiangiogenic compound might prove useful in treating corneal neovascular disease.

Ex vivo lentiviral transduction of rabbit Tenon's cells with subsequent reinjection of transduced cells was studied. Subconjunctival injection of cells transduced with lentiviral capable of expressing sKDR or sNRP-1 did not show statistical significance compared to controls in inhibiting corneal NV when observed during the first 10 postinjury days. However, on day 12 after initiation of corneal NV stimuli, the subjects that received Tenon's transduced with both transgenes (*sKDR* and *sNRP-1*) demonstrated statistically significant less NV. How sKDR and sNRP-1 act in a synergistic fashion to enhance the inhibitory effect of either soluble VEGF receptor alone in this particular model is not clear. The fact that this effect did not persist may be due to insufficient number of Tenon's cells injected into the subconjunctival space or that the cells did not long survive after injection. It is also possible that these heterologous implants elicited an immune response that ultimately cleared transgene-expressing cells. Further work will be necessary to explore subconjunctiva injection as a method of gene therapy of anterior segment neovascular diseases.

NaOH Injury Model

The fusion gene *MIG:IP10* was studied to evaluate its effect on angiogenesis associated with chemically induced corneal injury. The overall result was a decrease in severity of the injury response. There appeared to be very few basophilic infiltrates in treated corneas

when compared with controls. Considering that both MIG and IP10 proteins are related by function, it is possible that the overexpression of these genes effectively inhibited the normal immune response. In this model, there was also a reduction of invasive blood vessels to the wound site. It has been demonstrated that certain immune cells that have been recruited to a wound site can stimulate or themselves produce angiogenic modulators, such as VEGF.[37] By down-regulating the immune response, it may be possible to disrupt the process of neovascularization.

A replication defective lentiviral system was constructed that harbored the *TIMP-1* gene. The virus was shown to be capable of transducing endothelial cells in vitro. Initial data suggest that TIMP-1 is not a potent inhibitor of neovascularization in the NaOH injury model. There was a steady increase in the overall angiogenesis in both control and TIMP-1 treated corneas. However, RT-PCR studies of treated corneal tissue failed to reproducibly demonstrate transgene expression; expression was observed in one of three corneas. TIMP-1 is known to inhibit the degradation of extracellular matrices, which is thought to be required for progressive neovascularization. The failure to inhibit neovascularization in our model may simply represent a failure of efficient transduction or a failure to generate therapeutic TIMP-1 protein levels.

PKP Model

Treatment of corneal graft tissue with lentiviral Endo: Kringle5 prior to engraftment was able to prevent new vessel growth onto the donor graft in all treated corneas. Histologic study revealed a marked decrease in inflammation in Endo: Kringle5 treated corneas; this includes the areas around retained sutures, a commonly inflamed area. Furthermore, there was no evidence of graft failure, as measured by a lack of corneal edema and persistent corneal clarity in Endo: Kringle5 treated corneas, whereas five of six control corneas exhibited evidence of opacification and failure.

The ability to retard new blood vessel growth by the fusion protein Endo: Kringle5 might be augmented by its potentially bifunctional structure. Endostatin has been shown to inhibit new vessel growth in solid tumors in a rat hemangioendothelioma model.[38] Kringle-5 is a specific inhibitor of endothelial cell proliferation in bovine capillary cells and prevents migration of endothelial cells in a number of cell cultures stimulated by bFGF. Endostatin and angiostatin proteins given together have been shown to cause more regression of blood vessels and ovarian cancer cells in an experimental model than when administered individually.[39,40] Similarly, these two proteins given together as an Fc-Angiostatin plus Fc-Endostatin combination resulted in a significant reduction of tumor size in Ripa1-Tag2 mice, whereas given separately they had a markedly reduced effect.[41] Pretreatment of donor tissue in clinical situations at highest risk for graft failure may prove useful.

VEGF Retinal Edema Model

The retinal vascular leakage model employed intravitreal or subretinal injection of lentiviral particles into rabbit eyes in an attempt to modify the process of VEGF-induced vascular leakage in the New Zealand Red rabbit. The leakage induced by VEGF was transient in nature. Initial data suggest that KDR and/or sNRP-1 were capable of exerting a biologic effect by inhibiting leakage. By increasing the VEGF level, it was possible to overwhelm the competitive inhibition of KDR and sNRP-1. These reagents may prove useful in the treatment of VEGF-dependent macular edema, but further studies are required to fully validate these observations. It is of interest that there was no significant difference seen between groups that were administered virus to the vitreous or to the subretinal space.[42]

IN VIVO PRIMATE STUDIES

Most types of neovascularization within the adult eye will lead to visual impairment.[43] AMD is the leading cause of irreversible loss of vision in the elderly in the United States[44]; the development of SRN in patients with AMD is a major contributor to vision loss.[45] The data presented indicate that lentiviral mediated *K1-5* gene expression significantly blunts the vascular changes associated with laser disruption of Bruch's membrane in primates.

Each kringle (K) domain is about 80 amino acids long with 6-conserved cysteine residues, which contribute to the triple-loop disulfide structure. Each possesses different antiangiogenic potential. The exact mechanism of action of the K1-5 plasminogen fragment is not completely understood; however, analysis of individual K domains of plasminogen indicates that K1, K2, K3, and K5, but not K4, inhibit endothelial cell proliferation, and that K1-3 and K5 alone are more potent at inhibiting endothelial cell proliferation than angiostatin (K1-4).[46,47] Intravitreal injections of the K5 protein in a rat model of ocular neovascularization reduce disease progression with concurrent decrease in VEGF and an increase in PEDF mRNA and protein levels within the retina.[48] The K1-5 fragment contains complete K1-4 domains and a majority of the K5 domain (only five of the usual six cysteine residues).[49,50] Whether K1-5 can also up-regulate PEDF and decrease VEGF levels is not known; however, systemic administration of the K1-5 protein is significantly more potent at inhibiting basic fibroblast growth factor induced corneal neovascularization in a murine model when compared directly with the inhibitory effect of angiostatin (K1-4) in the same model.[49]

In this study, treatment efficacy was established at 6 months and again at 10 months after rechalleging the same eyes with nonoverlapping laser spots. The prevention of disease progression after rechallenge is of high significance, since SRN can often recur within the same eye after laser photocoagulation or photodynamic treatment for neovascular AMD with subsequent loss of vision.[51] Persistent therapy throughout the period of intraocular neovascular disease is desirable in many clinical settings, not only as a treatment but perhaps also as a preventative therapy. It is conceivable that inhibiting angiogenesis at different stages of this complex process may prove synergistic. Treatment with a combination of different genes, such as *TIMP-3* (an inhibitor of the matrix metalloproteinases, proteins involved in the degradation of the extracellular matrix), *K1-5*, or a soluble VEGF receptor, or with all three attacking different pathways of angiogenesis, merits study. This study concludes that the K1-5 fragment of human plasminogen delivered via a lentiviral vector can significantly ameliorate the progression of vascular leakage as seen in serial angiograms in a

primate model of SRN and may prove beneficial as an adjunct therapy for the exudative form of AMD.

The testing of various antiangiogenic genes delivered by a replication defective lentiviral system indicates that some gene products may be more potent at inhibiting ocular neovascularization disease than others. In addition, while the lentiviral delivery system is effective as a method of gene delivery in most cell types, some cells are more refractory to transduction and long-term transgene expression. We have established that a lentiviral system is viable vector for development and use for the management of ocular proliferative disease. Because several of the tested genes appear to be affective at blunting or abolishing the neovascular response, further study would seem warranted.

REFERENCES

1. Council on Scientific Affairs. Report of the organ transplant panel: corneal transplantation. *JAMA* 1988;259:719-722.
2. Gomez DE, Alonso DF, Yoshiji H, et al. Tissue inhibitors of metalloproteinases: structure, regulation and biological functions. *Eur J Cell Biol* 1997;74:111-122.
3. Bramhall SR, Stamp GW, Dunn J, et al. Expression of collagenase (MMP2), stromelysin (MMP3) and tissue inhibitor of the metalloproteinases (TIMP1) in pancreatic and ampullary disease. *Br J Cancer* 1996;73:972-978.
4. Docherty AJ, Lyons A, Smith BJ, et al. Sequence of human tissue inhibitor of metalloproteinases and its identity to erythroid-potentiating activity. *Nature* 1985;318:666-669.
5. Martin DC, Ruther U, Sanchez-Sweatman OH, et al. Inhibition of SV40 T antigen-induced hepatocellular in TIMP-1 transgenic mice. *Oncogene* 1996;13:569-576.
6. Soker S, Miao HQ, Nomi M, et al. $VEGF_{165}$ mediates formation of complexes containing VEGFR-2 and Neuropilin-1 that enhance $VEGF_{165}$-receptor binding. *J Cell Biochem* 2002;85:357-368.
7. Chibber R, Molinatti PA, Rosatto N, et al. Toxic action of advanced glycation end products on cultured retinal capillary pericytes and endothelial cells: relevance to diabetic retinopathy. *Diabetologia* 1997;40:156-164.
8. Stitt AW. The role of advanced glycation in the pathogenesis of diabetic retinopathy. *Exp Mol Pathol* 2003;75:95-108.
9. Yoon SS, Eto H, Lin CM, et al. Mouse Endostatin inhibits the formation of lung and liver metastases. *Cancer Res* 1999;59:6251-6256.
10. Shichiri M, Hirata Y. Anti-angiogenesis signals by Endostatin. *FASEB J* 2001;15:1044-1053
11. Lucas R, Holmgren L, Garcia I, et al. Multiple forms of angiostatin induce apoptosis in endothelial cells. *Blood* 1998;92:4730-4741.
12. O'Reilly MS. Angiostatin: an endogenous inhibitor of angiogenesis and of tumor growth. *EXS* 1997;79:273-294.
13. Yamaguchi N, Anand-Apte B, Lee M. Endostatin inhibits VEGF-induced endothelial cell migration and tumor growth independently of zinc binding *EMBO J* 1999;18:4414-4423.
14. Hanai J, Dhanabal M, Karumanchi SA, et al. Endostatin causes G1 arrest of endothelial cells through inhibition of cyclin D1. *J Biol Chem* 2002;277:16464-16469.
15. Troyanovsky B, Levchenko T, Mansson G, et al. Angiomotin: an angiostatin binding protein that regulates endothelial cell migration and tube formation. *J Cell Biol* 2001;152:1247-1254.
16. Ji W-R, Barrientos LG, Llinas M, et al. Selective inhibition by Kringle-5 of human plasminogen on endothelial cell migration: an important process in angiogenesis. *Biochem Biophys Res Commun* 1998;247:414-419.
17. Farber JM. Mig and IP-10: CXC chemokines that target lymphocytes. *J Leukoc Biol* 1997;61:246-257.
18. Sgadari C, Farber JM, Angiolillo AL, et al. Mig, the monokine induced by interferon-gamma, promotes tumor necrosis in vivo. *Blood* 1997;89:2635-2643.
19. Sgadari C, Angiolillo AL, Cherney BW, et al. Interferon-inducible protein-10 identified as a mediator of tumor necrosis in vivo. *Proc Natl Acad Sci USA* 1996;93:13791-13796.
20. Levy I, Paldi T, Shoseyov O. Engineering a bifunctional starch-cellulose cross bridge protein. *Biomaterials* 2004;25:1841-1849.
21. Schmidt-Wolf GD, Schmidt-Wolf IG. Non-viral and hybrid vectors in human gene therapy: an update. *Trends Mol Med* 2003;9:67-72.
22. Wells DJ. Gene therapy progress and prospects: electroporation and other physical methods. *Gene Ther* 2004;11:1363-1369.
23. McConnell MJ, Imperiale MJ. Biology of adenovirus and its use as a vector for gene therapy. *Hum Gene Ther* 2004;15:1022-1033.
24. Klonjkowski B, Denesvre C, Eloit M. Adenoviral vectors for vaccines. In: Seth P, ed. *Adenoviruses: Basic Biology to Gene Therapy*. Austin, Texas: RG Landes; 1999:163-173.
25. Romano G, Pacilio C, Giordano A. Gene transfer technology in therapy: current applications and future goals. *Oncologist* 1998;3:225-236.
26. Merten OW, Geny-Fiamma C, Douar AM. Current issues in adeno-associated viral vector production. *Gene Ther* 2005;12:51-61.
27. Buning H, Braun-Falco M, Hallek M. Progress in the use of adeno-associated viral vectors for gene therapy. *Cells Tissues Organs* 2004;177:139-150.
28. Lewis PF, Emerman M. Passage through mitosis is required for onco-retroviruses but not for the human immunodeficiency virus. *J Virol* 1994;68:510-516.

29. Levy JA, Conrat HF, Owens RA. Viruses using reverse transcription during replication. In: *Virology.* Upper Saddle River, New Jersey: Prentice Hall;1994:125-141.

30. Theoretical Biology and Biophysics Group. Landmarks of the genome. In: Kuiken C, Foley B, Hahn B, et al, eds. *HIV Sequence Compendium.* Los Alamos National Laboratory; 2000:v-viii.

31. Akkina RK, Walton RM, Chen ML, et al. High-efficiency gene transfer into CD34^{+} cells with a human immunodeficiency virus type 1-based retroviral Vector pseudotyped with vesicular stomatitis virus envelope glycoprotein G. *J Virol* 1996;70:2581-2585.

32. Simpson E. Immunotherapy and gene therapy. *Drugs* 2004;7:105-108.

33. Chinen J, Puck JM. Successes and risks of gene therapy in primary immunodeficiencies. *J Allergy Clin Immunol* 2004;113:595-603.

34. Flannery JG, Zolotukhin S, Vaquero MI, et al. Efficient photoreceptor-targeted gene expression in vivo by recombinant adeno-associated virus. *Proc Natl Acad Sci USA.* 1997;94:6916-6921.

35. Hematti P, Hong BK, Ferguson C, et al. Distinct genomic integration of MLV and SIV vectors in primate hematopoietic stem and progenitor cells. *PLoS Biol* 2004;2:e423.

36. Kuger EA, Durat PH, Tsokos MG, et al. Endostatin inhibits microvessel formation in the ex vivo rat aortic ring angiogenesis assay. *Biochem Biophys Res Commun* 2000;268:183-191.

37. Boesiger J, Tsai M, Maurer M, et al. Mast cells can secrete vascular permeability factor/vascular endothelial cell growth factor and exhibit enhanced release after immunoglobulin E-dependent up regulation of Fc epsilon receptor I expression. *J Exp Med* 1998;188:1135-1145.

38. O'Reilly MS, Boehm T, Shing Y, et al. Endostatin: an endogenous inhibitor of angiogenesis and tumor growth. *Cell* 1997;88:277-285.

39. Yokoyama Y, Dhanabal M, Griffioen AW, et al. Synergy between angiostatin and endostatin: inhibition of ovarian cancer growth. *Cancer Res* 2000;60:2190-2196.

40. Scappaticci FA, Smith R, Pathak A, et al. Combination angiostatin and endostatin gene transfer induces synergistic anti-angiogenic activity in vitro and anti-tumor efficacy in leukemia and solid tumors in mice. *Mol Ther* 2000;3:186-196.

41. Bergers G, Javaherian K, Lo KM, et al. Effects of angiogenesis inhibitors on multistage carcinogenesis in mice. *Science* 1999;284:808-812.

42. Cheng L. Human immunodeficiency virus type 2 (HIV-2) vector-mediated in vivo gene transfer into adult rabbit retina. *Curr Eye Res* 2002 24:196-201.

43. Lee P, Wang CC, Adamis AP. Ocular neovascularization: an epidemiologic review. *Surv Ophthalmol* 1998;43:245-269.

44. Varmus H. Age-related macular degeneration: status of research. Bethesda, Maryland: Department of Health and Human Service, National Institutes of Health, March 1997. Available at : http://www.nei.nih.gov/news/statements/varmus.htm. Accessed Dec 20, 2005.

45. Bressler SB, Maguire MG, Bressler NM, et al. Relationship of drusen and abnormalities of the retinal pigment epithelium to the prognosis of neovascular macular degeneration. The Macular Photocoagulation Study Group. *Arch Ophthalmol.* 1990;108:1442-1447.

46. Cao Y, Ji RW, Davidson D, et al. Kringle domains of human angiostatin, characterization of the anti-proliferative activity on endothelial cells. *J Biol Chem* 1996;271:29461-29467.

47. Cao Y, Chen A, An SS, et al. Kringle 5 of plasminogen is a novel inhibitor of endothelial cell growth. *J Biol Chem* 1997;272:22924-22928.

48. Gao G, Li Y, Gee, S, et al. Down-regulation of vascular endothelial growth factor and up-regulation of pigment epithelium-derived factor: a possible mechanism for the anti-angiogenic activity of plasminogen kringle 5. *J Biol Chem* 2002;277:9492-9497.

49. Coa R, Wu HL, Veitonmaki N, et al. Suppression of angiogenesis and tumor growth by the inhibitor K1-5 generated by plasmin-mediated proteolysis. *Proc Natl Acad Sci USA.* 1999;96:5728-5733.

50. Sumariwalla PF, Cao Y, Wu HL, et al. The angiogenesis inhibitor protease-activated kringles 1-5 reduces the severity of murine collagen-induced arthritis. *Arthritis Res Ther.* 2003;5:R32-39.

51. Macular Photocoagulation Study Group. Persistent and recurrent neovascularization after laser photocoagulation for subfoveal choroidal neovascularization of age-related macular degeneration. *Arch Ophthalmol* 1994;112:489-499